Salt-marsh reconstructions of relative sea-level change in the North Atlantic during the last 2000 years

Barlow, N.L.M.[1]*

Long, A.J.[1]

Saher, M.H.[2]

Gehrels, W.R.[2]

Garnett, M.H.[3]

Scaife, R.G.[4]

*Corresponding author: n.l.m.barlow@durham.ac.uk +44 (0)191 334 192

Keywords

North Atlantic; sea level; transfer function; diatoms; foraminifera; salt marsh; climate

Abstract

Sea-level changes record changes in the mass balance of ice sheets and mountain glaciers, as well as dynamic ocean-atmosphere processes. Unravelling the contribution of each of these mechanisms on late Holocene timescales ideally requires observations from a number of sites on several coasts within one or more oceans. We present the first 2000 year-long continuous salt marsh-based reconstructions of relative sea-level (RSL) change from the eastern North Atlantic and uniquely from a slowly uplifting coastline. We develop three RSL histories from two sites in north west Scotland to test for regional changes in sea-level tendency (a positive tendency indicating an increase in the proximity of marine conditions and a negative tendency the reverse), whilst at the same time highlighting methodological issues, including the problems of dataset noise when applying transfer functions to fossil salt-marsh sequences. The records show that RSL has been stable (±0.4 m) during the last two millennia, and that the regional sea-level tendency has been negative throughout most of the record lengths. A recent switch in the biostratigraphy of all three records, indicating a regional positive tendency, means we cannot reject the hypothesis of a 20th century sea-level acceleration occurring in north west Scotland that must have exceeded the rate of background RSL fall (-0.4 mm yr^{-1}), but this signal appears muted and later than recorded from the western North Atlantic.

1 Introduction

The challenge of understanding how sea level has varied in the last few thousand years is important for several reasons. Firstly, sea-level variability records the net effect of changes in the mass balance of polar ice sheets and mountain glaciers as well as dynamic ocean-atmospheric processes. Sea-level observations have the potential to unravel these mass contributions which manifest themselves in spatially unique patterns, or 'sea-level fingerprints' (Mitrovica et al., 2011). Secondly, long-term trends in sea level provide insights into climate variability during periods of warmer and cooler periods in the past, such as the Medieval Climate Anomaly or the Little Ice Age (Cronin, 2012). Thirdly, past sea-level records are useful to test and develop models of ice-sheet response to past climate change and models of glacial isostatic adjustment (GIA).

Despite their importance, there are surprisingly few precisely dated, continuous records of sea-level change covering last 2000 years; indeed many existing records are discontinuous or have large vertical or temporal gaps (as summarised in databases such as Engelhart and Horton, 2012; Shennan and Horton, 2002). Continuous records of sea-level change are arguably best developed from low energy salt-marsh deposits that fringe mid latitude coastlines. Although the number of such studies is increasing (see Long et al., 2014) there are only a few near-continuous 2000-year long salt-marsh records: three from the western North Atlantic (Maine, North Carolina and New Jersey, USA; Gehrels, 1999; Kemp et al., 2011; Kemp et al., 2013 respectively) and one from Iceland (Gehrels et al., 2006a) (Figure 1). One of the most complete records from the European margin is a discontinuous series of basal and intercalated index points from Ho Bugt, Denmark (Gehrels et al., 2006b; Szkornik et al., 2008). The salt-marsh records presented in Figure 1 differ in their timing, direction and magnitude of RSL change, suggesting local to regional-scale patterns. Better understanding of the ways that sea level responds to different forcing factors requires additional records from elsewhere in the North Atlantic and beyond, before their significance can be firmly established.

Here we present the first continuous 2000 year-long records of relative sea-level (RSL) change from the eastern North Atlantic, from two salt marshes located in north west Scotland, UK (Figure 2). These sites record long term RSL fall caused by glacio-isostatic uplift. This contrasts with the existing late Holocene RSL records that are from subsiding sites where sea-level accelerations are potentially harder to define (e.g. Donnelly, 2006; Gehrels et al., 2004; Kemp et al., 2011; Kemp et al., 2013; Long et al., 2014; Szkornik et al., 2006). In this paper we test the hypothesis that the salt marshes in north west Scotland do not record a change in the sign of sea level from negative to positive during the last 2000 years.

2 Background

Along the northeast coast of the USA, two salt marsh sea-level records identify late Holocene phases of sea level rise and fall. Kemp et al.'s (2011) North Carolina salt-marsh reconstruction shows four phases of RSL change over the last 2000 years (Figure 1): a period of stable sea level from ~BC 100 to AD 950; a rise (0.6 mm yr^{-1}) in sea level from ~AD 950 to AD 1375; stable, or slightly falling, sea level from ~AD 1375 to the late 19^{th} century; and a period of rapid sea-level rise (2.1 mm yr^{-1}) from the late 19^{th} century to present. A complementary record from New Jersey (Kemp et al., 2013) shows asynchronous changes compared to the North Carolina record prior to the late 19th century sea-level rise, with sea level falling at 0.1 mm yr^{-1} prior to ~AD 230, followed by a rise of 0.6 mm yr^{-1} until ~AD 730, when RSL falls slightly at 0.1 mm yr^{-1} until the mid-19^{th} century rise of 3.1 mm yr^{-1} (Figure 1). Shorter (~1000 years) records from Maine (Gehrels et al., 2002) and Nova Scotia (Gehrels et al., 2004) similarly record local to regional RSL signals prior to rapid rates of 20th century RSL rise. Basal and intercalated sea-level index points also record late Holocene RSL changes along the western Atlantic margin (Engelhart and Horton, 2012), though due to their noncontiguous nature they are unable to resolve century-scale fluctuations in RSL of less than ~50 cm. Datasets which cover the last 700 and 1500 years in Connecticut, USA (Donnelly et al., 2004; van de Plassche, 2000 respectively) and AD 600-1600 in Louisiana (González and Törnqvist, 2009) provide snapshots of past RSL, but it is difficult to clearly identify periods of past sea-level change from such short records. It has been suggested that the regionally variable signals along the USA-Canadian margin during the late Holocene may, in part, be due to changes in the strength and position of the Gulf Stream (Fairbridge, 1992; Fletcher et al., 1993; Gehrels et al., 2002), in a similar way to sea-level changes recorded by tide gauges over the last 50 years (Kopp, 2013; Sallenger et al., 2012).

Outside of the USA there are very few continuous palaeo-records from the North Atlantic. A ~2000 year detrended salt-marsh reconstruction from Iceland shows a period of RSL rise prior to ~AD 450 followed by RSL fall prior to the recent acceleration (Gehrels et al., 2006a) (Figure 1). Late Holocene RSL reconstructions from the eastern Atlantic margin are currently restricted to 150-300 year long records (Leorri and Cearreta, 2009; Rossi et al., 2011) which show muted rates of recent RSL rise when compared to the western margin (Long et al., 2014), and non-continuous basal and intercalated index points (e.g. Baeteman et al., 2011; Edwards, 2001; Horton and Edwards, 2005; Szkornik et al., 2008) (Figure 1).

One of the challenges of deciphering the spatial and temporal patterns of late Holocene sea-level fluctuations is removal of the local long-term RSL signal against which the fluctuations occur. This signal is a consequence of ongoing postglacial land-level change (GIA) and geoid deformation (Shennan et al., 2012). Existing approaches to isolate this signal involve calculating rates of RSL using basal sea-level index points that are collected from above an uncompressible substrate and that are unaffected by compaction, which is then subtracted from the salt-marsh record (Gehrels et al., 2006a; Kemp et al., 2011). These basal sea-level index points typically have relatively large chronological and altitudinal uncertainties compared to contiguous, up-core salt-marsh records, which can add to the uncertainty of the "detrended" record.

During the late Holocene, the British Isles have experienced land uplift in Scotland and northern England (between 0-2 mm yr^{-1}), and subsidence in southern England (between 0 and -2 mm yr^{-1})

(Bradley et al., 2011; Shennan and Horton, 2002) (Figure 2A). The field sites reported here are from northwest Scotland and are chosen because they have experienced slight RSL fall during the late Holocene. The rate of RSL fall is currently modelled at ~-0.4 mm yr^{-1} (Bradley et al., 2011), though it is difficult to know if this rate was constant for the last 2000 years. We rely on estimates of land-uplift from GIA models as there very limited Holocene sea-level index points from northwest Scotland (Shennan and Horton, 2002). Therefore, there is some uncertainty as to the exact value of current day land-level change, though the general spatial pattern of post-LGM land-level change in Britain is reasonably well understood (Bradley et al., 2011; Smith et al., 2012). The RSL fall in north west Scotland is in contrast to other late Holocene RSL records in the North Atlantic from coastlines that are isostatically subsiding. We use these GIA contrasts to test for changes in the local and regional 'tendency' and the rate of change in RSL in northwest Scotland and compare it to the other multi-millennial records. The 'tendency' of a sea-level data point describes whether the litho- and bio-stratigraphy associated with the point records an increase or decrease in the proximity of marine conditions. Local tendencies are specific to a single site and may record a change in the rate of sea level, or a local change in coastal morphodynamics, whereas regional tendencies that occur in several sites are more likely to record changes in the regional rate of sea level. It is a helpful means of analysis, since on uplifting coastlines, where the background sea-level tendency will be negative, reversal of the signal may signify the dominance of a non-GIA signal such as ocean or atmospheric forcing, especially if recorded at more than one site in different morphodynamical settings. The opposite case applies to changes in tendency on subsiding coastlines. Mindful that these Scottish sites have experienced long term RSL fall at a modelled rate of ~-0.4 mm yr^{-1} (Bradley et al., 2011), any multi-decadal late Holocene sea-level rise that exceeds 0.4 mm yr^{-1} should be expressed as change to a positive regional tendency, circumventing the uncertainties associated with detrending the RSL reconstructions to remove background GIA.

3 Field sites

The salt marshes that are the focus of this study are located at the head of two remote fjords in Sutherland (Figure 2). The coastline is sparsely populated (1.1 persons km^{-2}) with no obvious modern on-site human disturbance. We focus on two sites with salt-marsh sediments up to 1 m thick at Loch Laxford and the Kyle of Tongue, ~27 km south and ~36 km east of Cape Wrath respectively (Figure 2B).

3.1 Loch Laxford

Loch Laxford is ~7 km long, ~1.2 km wide and includes two subsidiary lochs (Loch Dughaill and Loch a' Chadh-fi) (Bates et al., 2004) (Figure 2C). The outermost part is exposed to prevailing westerly winds, but at the loch head a sheltered inlet leads to a small basin, Tràigh Bad na Bàighe, with a sand-dominated tidal flat and vegetated salt marsh that abuts steep topography of Lewisian Gneiss Complex metamorphic rocks (Johnston, 1989). A small salt-marsh cliff, ~10 cm, forms the boundary between sand flat and salt marsh across much of the site. *Armeria maritima* (thrift) dominated salt marsh supports an extensive creek network, and covers ~1.2 m vertical elevation range, with an uppermost zone of freshwater *Iris* that grades landwards into heather upland communities. The spring tidal range is 4.3 m (Table 1). A transect of 13 hand-cores across the marsh (Figure 3), as far away from the creek network as possible, records a sequence of homogenous silty peat which progressively shallows seaward, overlying firm intertidal sand. Material was collected for detailed analysis from locations LA-3 and LA-6 (core top elevation 2.11 and 1.80 m OD respectively).

3.2 Kyle of Tongue

Kyle of Tongue (Figure 2D) is ~12 km long, ~1.7 km wide and largely bounded by metamorphic rocks of the Lewisian and Morar groups (Johnston, 1989). At its head, the Kinloch and Allt Ach 'an t Srathain rivers discharge into the sea and several areas of salt marsh have developed, with the largest area (~300 x 95 m) situated between the two river mouths (Figure 2). Much of the marsh front is eroding with a ~1 m high face and large blocks of eroded marsh deposit on the tidal flat, but there are nevertheless a few areas of transitional succession from sand flat to *F. cottonnii* salt marsh, through to *Carex* high marsh and *Calluna vulgaris* heathland. Vegetated salt marsh covers a ~1.4 m vertical range. The spring tidal range is 4.4 m (Table 1). A transect of eight hand-cores across the marsh plus cleaning of a face section (Figure 3) records a progressively seaward deepening sequence. We selected location KT-3 (core top elevation 2.62 m OD) for further laboratory analysis as it avoided the 'pinching out' of the organic horizons (Figure 3).

4 Methods

4.1 Laboratory methods

We prepared the fossil sediments for a range of lithological, microfossil and chronological analyses to allow us to develop reconstructions of past sea level. Duplicate cores were collected at each site using an 8 cm wide hand gouge and, in the case of KT-3, additional near-surface material using a trenching spade to cut a large sediment block and wrapped it in plastic. Organic content was measured as percentage loss on ignition (LOI), by burning ~5g of dried sediment at 550^{o}C for four hours.

Samples for diatom and foraminifera analysis were prepared following standard techniques (Moore et al., 1991; Palmer and Abbott, 1986) with 250 diatom valves counted in all samples and a minimum of 69 and 75 foraminifera tests counted (average: 164) in the fossil and modern samples, respectively, except where test concentrations were too low to sustain such numbers. The foraminifera assemblage has a low species diversity (4 and 7 species in the fossil and modern samples, respectively) which allows for lower total counts (Fatela and Taborda, 2002). The foraminiferal assemblages in both Loch Laxford cores comprise >90% *Jadammina macrescens* in most samples, with low occurrences of *Trochammina inflata* and *Miliammina fusca*. This (almost) monospecific assemblage provides little information regarding changes in marsh-surface elevation, but helpfully confirms the identification of salt-marsh facies throughout the cores. As a result, we focus our analyses at both sites on diatoms which have more diverse assemblages and which we interpret using a large (215 samples) modern diatom database from north west Scotland, which includes samples from Loch Laxford and Kyle of Tongue, as well as seven other salt marshes from the west coast of Scotland (Barlow et al., 2013). We present fossil diatom data from every 1-2 cm depth, ensuring samples are counted for every dated level and at 1 cm resolution for the last 200 years.

Pollen sub-samples were taken at an interval of 2 or 4cm depending on desired resolution. Pollen was moderately abundant and largely well preserved throughout and counts of 300-400 grains per sample to be identified and counted. A standard pollen diagram was constructed using Tilia and Tilia Graph.

We develop a chronology using ^{14}C, ^{210}Pb, ^{137}Cs, pollen, lead isotopes and metal pollutant horizons. A lack of macrofossil preservation at both sites means Accelerator Mass Spectrometry (AMS) ^{14}C dating of plant macrofossils was not possible (with the exception of the top 8 cm at KT-3) and so the radiocarbon chronology is, therefore, based on AMS ^{14}C dating of bulk sediment samples. After four initial ^{14}C dates from 15, 30, 45 and 60 cm in LA-3, the *R-simulate* function in OxCal (Bronk Ramsey, 2001) was used to target depths that, where possible, avoided plateaus in the ^{14}C calibration curve. AMS dating of bulk samples focused on the humin fraction, that is, the organic component that is insoluble in water at all pH values, and excludes mobile decomposing soil organic matter and humic acids which can result in younger ^{14}C ages (Balesdent, 1987). To test for potential contamination, we dated paired humin and humic fractions from bulk samples taken from 4 sample depths in LA-3, and compared humin fraction results to plant macrofossil dates in the upper 8 cm of KT-3.

All ^{14}C samples were prepared to graphite targets at the NERC Radiocarbon Facility (East Kilbride, UK). For bulk sediment samples, the humin fraction was isolated using acid-alkali-acid extraction, whereas the small number of macrofossil samples was subjected to an acid wash. All samples were combusted to CO_2, cryogenically purified and converted to graphite by Fe:Zn reduction. Radiocarbon measurements were performed by AMS at the Scottish Universities Environmental Research Centre (East Kilbride, UK). In an attempt to maximize the resolution of the ^{14}C chronology many samples were measured as multiple graphite targets (when availability of sample material allowed) and some were selected for high precision AMS. Following convention, all ^{14}C results are normalised to a $\delta^{13}C$ of -25 ‰, and expressed as % modern and conventional radiocarbon ages (in years BP, relative to AD 1950).

We dated the top ~10 cm of the sample cores using the radioactive isotopes ^{210}Pb and ^{137}Cs. ^{210}Pb is a naturally occurring radionuclide with a half-life of 22.3 years which provides chronological control on the last 100-150 years of sediment deposition (Robbins, 1978). ^{137}Cs is an artifact of the atmospheric testing of nuclear weapons post AD 1950, with the peak deposition occurring in AD 1963. Preparation of 1 cm thick, contiguous samples, followed standard techniques with the energies of each isotope measured using Ortec p-type Series Germanium gamma ray spectrometers at Durham University, and development of a simple ^{210}Pb age-depth model for each profile (Appleby and Oldfield, 1983).

Salt marshes can act as heavy metal sinks and regional and local contamination can result in distinct chronological horizons (e.g. Cundy and Croudace, 1995; Cundy et al., 1997), with ratios of stable isotopes $^{206}Pb/^{207}Pb$ having the potential to identify regional and global sources of pollution (Komarek et al., 2008). To assess the potential of such pollutant records at Loch Laxford and Kyle of Tongue we used a Perkinelmer ELAN DRC single-quad Inductively Coupled Plasma Mass

Spectrometer (ICP-MS) at Durham University to measure a suite of elements and Pb isotopes in LA-3 in an attempt to identify the onset of industrial atmospheric pollution, following standard preparation techniques of 1 cm slices of sediment. The results (supplementary information Figure 1) show a decrease in $^{206}Pb/^{207}Pb$ in the top of the core, similar to that of Kylander et al. (2009) from a blanket bog ~15 km inland of the Loch Laxford salt marsh. The magnitude of the error term relative to the signal means the $^{206}Pb/^{207}Pb$ results provide no value over the ^{210}Pb data as the exact timing of the onset of industrialization in the record is hard to define. We are unable to identify any clear chronological markers in the elemental analyses, including when normalised against aluminum or lithium. Therefore, we did not pursue elemental or $^{206}Pb/^{207}Pb$ isotope analysis for the other cores.

From the resulting data we have developed an age-depth model for the three sequences using the Bayesian Markov chain Monte Carlo (MCMC) based age-depth modeling package, Bacon, in the open-source statistical environment, R (Blaauw and Christen, 2011), and the calibration curve IntCal09 (Reimer et al., 2009), by combining the ^{137}Cs, ^{210}Pb and the humin ^{14}C dates (see 5.3). We combine dates where pre-bomb ^{14}C samples have been dated in triplicate (i.e. the same sample analysed three times after graphitization) into a mean pooled radiocarbon age in Calib 6.1.1 (Stuiver and Reimer, 1993) before including in Bacon so as to avoid undue weight being placed on these samples.

4.2 Quantitative sea-level reconstructions

We develop a diatom transfer function, using the regional modern Scottish diatom training set from Barlow et al. (2013), to produce quantitative sea-level reconstructions at both sites. The transfer function models the relationship between modern diatom assemblages and elevation (supplementary information Figure 2). As reported in Barlow et al. (2013) the most accurate and precise model results are generated using the regional Scottish training set. The model is used to transform the fossil diatom assemblages into palaeomarsh-surface elevations (PMSE) in the tidal frame at the time they were deposited, with an associated (1σ) error term. We convert this PMSE to relative sea level using the following equation (note, Ordnance Datum (OD) is the national leveling datum for the UK):

RSL (m) = Depth (m OD) – Reconstructed palaeomarsh surface elevation (m OD)

Each transfer function model has specific choices and underlying statistical assumptions which can impact on the resulting reconstructions (Barlow et al., 2013; Birks, 1995) and therefore it is important to assess whether the results are both accurate and robust. We apply the modern analogue technique (MAT) to assess the latter by quantifying the similarity between each fossil sample and the modern training set (Birks, 1995). We use the 20th percentile of the minimum dissimilarity coefficients (MinDC) calculated between all modern samples as the cut-off between 'good' and 'poor' modern analogues (Watcham et al., 2013). These thresholds are used for visual guidance only. The reconstructed PMSE of the core top sample is also checked against its known elevation and we assess whether the reconstructions make sense compared to the stratigraphy.

5 Results

5.1 Lithology

The Loch Laxford lithostratigraphy (Figure 3) comprises a homogeneous silty peat of salt-marsh origin which thins seaward and overlies dense intertidal sand. The Kyle of Tongue transect similarly reveals a sequence with salt-marsh peat that overlies a dense organic silt (Figure 3), but which is underlain by a darker silty sand. Loss-on-ignition (LOI) data show that overall each sequence records an increase in organic content up core (Figures 4, 5 and 6), though an exception is seen in LA-6, where at ~58 cm and 25 cm the organic content falls briefly and suggests a more complex stratigraphy.

5.2 Biostratigraphy

5.2.1 Diatoms

The cores contain diverse salt-marsh diatom assemblages that include marine, brackish, and salt-water tolerant taxa (Figures 4, 5 and 6). We sort these fossil diatoms into groups that reflect different salinity tolerances using the bootstrapped weighted averaging partial least squared (WA-PLS) coefficient calculated from the modern dataset (supplementary information Figure 3). LA-6 shows relatively little change up core (Figure 5), although at 22 cm *Caloneis borealis* replaces *Diploneis ovalis* in importance, and there is an increase in an unidentifiable small *Navicula* sp. (Laxford) at ~4 cm. In contrast there are clear up-core changes in the diatom assemblages in LA-3 and KT-3 (Figures 4 and 6), most notably a replacement of marine by brackish water species. As in LA-6, there is an increase in the abundance of an unidentifiable *Navicula* sp. (Laxford) in LA-3 above ~4 cm. In summary, these results suggest LA-3 and KT-3, when viewed over the length of their records, are regressive sequences, dominated by an up-core reduction in marine influence and therefore negative local sea-level tendencies, with LA-6 recording relatively little change.

5.2.2 Foraminifera

Foraminifera were examined from the two Loch Laxford sample cores. Each profile is dominated by *Jadammina macrescens* with lesser frequencies of *Miliammina fusca* and *Trochammina inflata*. The assemblages confirm that the deposits formed in relatively stable salt-marsh conditions. We note that in the upper levels of core LA-6, the lower and more seaward of the two sample cores, there is an increase in the frequencies of *T. inflata*, *M. fusca* and *Haplophragmoides wilberti* above ~5-6 cm that records a slight lowering of the marsh surface relative to the tidal frame. A slight dip in frequencies of *T. inflata* also occurs in the LA-3 above 2-3 cm. The comparatively poor species diversity of the foraminifera compared to the diatom data meant that we did not examine any fossil foraminifera at Kyle of Tongue as they will not provide any additional quantitative constraint on palaeo-salt marsh elevation.

5.2.3 Pollen

Pollen analysis was undertaken through LA-6 to establish the character of on-site vegetation and identify possible biostratigraphical markers. The pollen sequence is largely homogeneous (supplementary information Figure 4) with, however, two apparent phases (local pollen assemblage zones). Throughout the profile, there is clear evidence that halophytes (salt-marsh plants) are present. These include *Plantago maritima* (sea plantain) with high values especially in the lower part of the sequence and *Armeria* types (thrift and sea lavender) which, given that they are poorly represented in pollen spectra, are especially important in the upper levels. Overall, these principal taxa indicate that the salt marsh was becoming drier. The allochthonous, regional pollen component is also represented showing presence of *Betula* (birch) and *Corylus avellana* type (including hazel and/or bog myrtle) and heathland elements (heather and ling). *Pinus* (pine) starts to increase in importance from *c.* 20cm and represents the introduction of plantations within the broader region.

5.3 Age models

The absence of plant macrofossils below ~10 cm in the sample cores required us to use bulk AMS ^{14}C dates. To test for possible age differences between different organic fractions, we dated four paired humin-humic samples from the LA-3. The results (Table 2) show that the humic fraction is younger than the equivalent humin fraction and that this difference increases down-core to 45 cm, below which the difference remains ~250-400 ^{14}C yr.

In the top of KT-3 we identified sufficient material to date paired seed/humin samples from two levels at 5.25 ± 0.25 cm and 6.75 ± 0.25 cm (Table 2). The sediments at this shallow depth straddle the pre- and post-(atomic) bomb periods. Both plant macrofossil samples have pre-bomb ^{14}C concentrations. However, the humin samples both have ^{14}C concentrations greater than 100%

modern, and therefore show the presence of post-bomb ^{14}C. We suspect this is caused by the downward penetration of fine rootlets that have mixed with pre-bomb carbon. As many of these roots as possible were removed in the laboratory prior to dating, but some may have decayed beyond visible recognition. The macrofossil and humin samples could differ in age by only a decade or two, but because of the form of calibration curve from AD 1930, calibration of these samples is overly sensitive to small changes in ^{14}C. Moreover, we note that the calibration of post-bomb humin samples can produce narrow age ranges though they likely contain both pre- and post-bomb 14C due to the low sedimentation rate (based upon the other dating evidence, a 1 cm sediment slice probably formed over 8-10 years). Notwithstanding these points, we cannot conclusively show from this test that the humin and macrofossil dates are the same age. However, in the absence of further material for paired macrofossil/humin dates, and the paired humic-humin dates (Table 2) producing the expected pattern of the humic fractions being younger than the humin component, we pursue the use the ^{14}C results from the humin fractions for the three sample cores.

Our age-depth models combine ^{137}Cs, ^{210}Pb and ^{14}C dates in each core. At Loch Laxford the Bacon model for the main core, LA-3 (supplementary information Figure 5), yields a linear regression of 0.29 ± 0.0043 mm yr^{-1}. The dates from ≥60 cm in LA-3 come from a silty sand and humified organic material (Figure 3). The spread of dates from this stratigraphic unit is likely due to mixing of tidal flat/low marsh sediments and for this reason we exclude dates from this unit in the RSL reconstruction.

The age-depth model for LA-6 is more complex (supplementary information Figure 6). The results suggest two periods of rapid sedimentation separated by a hiatus around 20-24 cm. The location of this hiatus corresponds with the fall in organic content to ~5% at 25 cm noted above and to an increase in the sand content at this part of the core (Figure 5). The lithostratigraphy at Loch Laxford shows that LA-6 is located towards the seaward limit of a thick peat sequence (Figure 3). We hypothesise, based on the age and sedimentological data reported above, that this stratigraphic change records a period of erosion ~AD 1500 ± 100 when the active marsh front was at, or close to, the position of LA-6, with the marsh front then prograding seawards once more in the subsequent half millennium. This complex sedimentation pattern is not evident in the biostratigraphy which suggests uninterrupted accumulation. For this reason, only the top 20 cm of the LA-6 core for is used for reconstructing RSL. The patterns described above caution against over-reliance on continuous biostratigraphy to infer uninterrupted sediment accumulation.

The sample cores from Kyle of Tongue yield broadly similar age models to LA-3. KT-3 (supplementary information Figure 7) has a linear rate of 0.35 ± 0.0035 mm yr^{-1}, with a few minor fluctuations. We note a good fit between the ^{14}C dates and ^{137}Cs and ^{210}Pb data, with the exception of the two ^{14}C samples at 12 and 20 cm which both contain modern carbon (Table 2), likely due to the factors discussed above. These modern dates are excluded from the KT-3 age model. As in LA-3, dates from below 50 cm in KT-3 come from a silty sand that contains humified organic material (Figure 3) and likely also some reworked carbon. We likewise exclude the dates from ≥50 cm in KT-3 from the RSL reconstructions.

5.4 Quantitative relative sea-level reconstructions

We use the north west Scotland WA-PLS regional 'coastal transition' model from Barlow et al. (2013) to calibrate the fossil diatom assemblages in the three cores. This model produces the most reliable results, compared to the other models, due to its long environmental gradient and greater species turnover (4.08 SD units), with 1σ errors of ~10% of the tidal range. An increase in PMSE up core in both LA-3 (Figure 4) and KT-3 (Figure 6) follows the regressive litho- and bio-stratigraphy. MAT MinDC values for both Loch Laxford cores are below the 20th percentile threshold (118), with a few samples in KT-3 having MinDCs slightly greater. The majority of these 'poor' samples come from below 50 cm which is excluded from the RSL reconstruction due to the poor dating control. Samples from 6-10 and 13-17 cm also slightly exceed the 20th percentile threshold meaning that the accuracy of this part of the record may be compromised. Therefore, it is particularly important to compare the AD 1700-1900 part of the records at all three sites for regional consistency. The PMSE reconstruction and associated error for the core top sample from all three cores overlaps the surveyed core top elevation.

To check for reproducibility of the transfer function results, we counted an extra 24 diatom samples from four six-cm deep profiles from a sediment block collected from next to KT-3 (Figure 7). As Turner et al. (1989) show in regards to pollen, overall trends in microfossils may be similar but a degree of random variation is expected even in samples taken very close to each other. Transfer function results consist of a reconstructed PMSE and a sample specific bootstrapped RMSE (1σ) term. Over-reliance on the mid-point of any RSL reconstruction may produce quite different conclusions as to the nature of RSL even though specific changes may simply be a consequence of local noise in the dataset. We plot reconstructed RSL for five samples at each depth (0-6 cm) against the KT-3 age model (Figure 7). There is a spread in the reconstructed elevation of the samples at each point, as a result of local noise in the fossil diatom dataset. However, the 1σ errors of the data points overlap, giving confidence in the reproducibility of the results and the trend of the overall signal. We also compare the results to the Aberdeen tide gauge with a 9-year moving average smoothing (Figure 7). (Although Kinclochbervie is the closest tide gauge, the record only starts in AD 1991 and has several data gaps). GIA modeling suggests that present day rates of RSL change are ~-0.6 mm yr^{-1} at Aberdeen and ~-0.4 mm yr^{-1} at Kyle of Tongue (Bradley et al., 2011), but these differences are not sufficiently great to cause the instrumental record to sit outside errors of the reconstruction over the timescale considered.

To assess that the reconstructed RSL changes in each core are independent of the age-depth model, we first plot the reconstructed RSL against depth (cm) and then compare the shape of the curves to the reconstructed elevations plotted against years (AD) (Figure 8). In all three instances the age-depth model does not generate inflections in the sea-level curve in addition to that recorded by the biostratigraphy, providing confidence that the reconstructed RSL changes are not an artifact of the limitations of our dating methods. The reconstructions show that the KT-3 record plots slightly higher, and therefore shows slightly greater RSL fall than the reconstruction from LA-3. This may be a consequence of slight differential long-term RSL between the two sites, as suggested by the GIA modeling predictions of Bradley et al. (2011) (Loch Laxford: -0.46 mm yr^{-1}; Kyle of Tongue: -0.48 mm yr^{-1}). Despite the local noise in each dataset and the non-analogue issues in the AD 1700-1900 part of the KT-3 core, both records allow us to test the hypotheses of late Holocene sea-level changes in north west Scotland.

6 Discussion

6.1 Late Holocene sea-level changes in north west Scotland

We chose field sites in north west Scotland because they have experienced slow RSL fall during the late Holocene due to GIA rebound, meaning that any rises in sea-level must exceed this signal (modelled rate of ~-0.4 mm yr^{-1} (Bradley et al., 2011)) if they are to be identified in the litho- and biostratigraphy of the sample cores. This contrasts with other late Holocene salt-marsh reconstructions (Figure 1), where subsidence dominates and positive sea-level tendencies are the norm. Furthermore, because GIA is a gradual, long-term process, it cannot be the driver of century-scale RSL fluctuations. For these reasons, we do not remove the long term GIA-dominated signal from the records from north west Scotland, also noting that depending on the value of the GIA correction used, rates of 'detrended' sea-level can either amplify or dampen rates of sea-level change experienced at a specific location (e.g. Grinsted et al., 2011).

Because of the issue of reworking in the age models for the deeper parts of the sample cores, our new RSL reconstructions start from AD 200 and AD 450 at Loch Laxford and Kyle of Tongue respectively (Figure 8). The trend of PMSEs in the two main cores (Figures 4 and 6) show a gradual emergence relative to the tidal frame with an increase in organic content of the cores (and the marsh more widely) as flooding frequencies fall. The trends in the diatom biostratigraphy in these records are consistent with these data.

We apply a smoothing function of ~50-60 years to test for multi-decadal changes in the sign of local sea-level reconstructions (e.g. a switch from negative (falling) to positive (rising) RSL) (Figure 8). To reject the hypothesis that the salt marshes in north west Scotland did not record a change in the sign of sea level from negative to positive during the last 2000 years requires identification of ubiquitous changes in the sign of RSL at both Loch Laxford and Kyle of Tongue.

Prior to the 20th century none of the fluctuations at each site are replicated at the other, meaning the reconstructed RSL changes are local in nature. However, within the latter part of all three records there is a consistent increase in RSL ~AD 1945-1980 (marked by the red arrows on Figure 8). The evidence does not point towards a strong change in sign; and indeed, a linear trend adequately summarises the RSL reconstructions from all three records from the start of the 19th century through to the present (Figure 9). However, closer inspection of the biostratigraphy from each record suggests a change from a negative to a positive local sea-level tendency happened around this time. Previously unrecorded diatom species appear in the top ~6 cm of the cores (e.g. an unidentifiable *Navicula sp*. (Laxford) in Loch Laxford (Figures 4 and 5); and *Denticula subtilis, Nitzschia microcephala* and *Nitzschia tryblionella* in KT-3 (Figure 6)) suggest a change in environment at this time. The foraminiferal data from the two Loch Laxford cores also suggest that the long-term negative sea-level tendency and marsh emergence was reversed in the last century, as indicated by the decline in frequencies of *J. macrescens* and by an increase in *T. inflata* in LA-3 and of both *M. fusca* and *T. inflata* in LA-6 in the top ~6 cm of each core. This signal is stronger in LA-6, which sits lower within the tidal frame. We do not believe this trend is a consequence of sediment compaction as Brain et al. (2012) show that records from shallow (<0.5 m) uniform-lithology stratigraphies, or shallow near-surface salt-marsh deposits in regressive successions, experience negligible compaction. The trend of a positive tendency in KT-3 appears to be reversed around AD 1980; this may be a consequence of the bridge and causeway which were built across the Loch in AD 1971 which most likely modified local sedimentation and tidal patterns.

Taken together, the results described above mean it is not possible to reject the hypothesis of a switch from a negative to a positive sea-level tendency at both sites from the mid-20th century onwards that is regional in origin. Although the age/altitude data are best approximated by a linear trend during this period, the age and height uncertainties of the individual data points may mask more subtle changes in the rate of sea-level change that are associated with the change in sea-level tendency indicated by the biostratigraphic data at two sites separated by ~40 km. We note that the background rate of GIA in Scotland means that if this change in tendency is caused by a regional sea level rise then it must have exceeded ~0.4 mm yr^{-1} to reverse the trend of negative sea-level tendency that prevailed during much of the previous millennium. Notably, our records provide no evidence for any other changes in regional tendency and therefore, no indication of significant sea-level rise or fall >0.4 mm yr^{-1} in north west Scotland during the previous 15-18 centuries.

We must also give consideration to the period of erosion the Loch Laxford marsh experienced ~AD 1500 ± 100. An equivalent positive tendency is potentially visible in LA-3 (Figure 4), where there is a slight drop in the long-term LOI trend, but nothing is obvious in the Kyle of Tongue records. Therefore, this local change in coastal morphodynamics, perhaps related to a change in sediment supply or a period of storms, should not be interpreted as evidence for a regional change in sea level. The timing of this erosive phase fits with a chronology of increased sand deposition from AD ~1400-1700 from the Outer Hebrides, west of Loch Laxford, which is argued to reflect periods of increased storminess in the Atlantic associated with increased sea ice cover and an increase in the thermal gradient across the North Atlantic region (Dawson et al., 2004) or alternatively it could be a consequence of more intense, rather than more frequent, storms during the Little Ice Age (Trouet et al., 2012). The westerly orientation of Loch Laxford, as supposed to the northerly Kyle of Tongue (Figure 2), means that this site may be more prone to North Atlantic storms from predominantly westerly winds, though the salt marsh in the Tràigh Bad na Bàighe basin has some shelter.

6.2 Comparison with late Holocene sea-level records from the North Atlantic

Three other 2000-year continuous salt-marsh records from the North Atlantic show several phases of local or regional RSL change (Figure 1), the most marked of which is the late 19th/early 20th century acceleration noted above. Our new results support the hypothesis of Long et al. (2014) that this recent acceleration is muted along the eastern North Atlantic margin (European coast) compared to the west (North American coast) (Figure 9). Although the biostratigraphy suggests that a mid-20th century change in sea-level tendency occurred, any associated change in the rate of RSL was too small in amplitude or too short in duration relative to the errors in the reconstructions to be notably discernible from what is a long-term, linear trend (Figure 9). The Aberdeen tide gauge is the longest in Scotland (from AD 1862) and it records an overall rise in the AD 1862-2006 period of 0.87 ± 0.1 mm yr^{-1}. It too records only a very slight 20th century acceleration (0.0062 ± 0.0016 mm yr^{-2}) (Woodworth et al., 2009).

An alternative interpretation of our Scottish data is that because they are located in uplifting areas, they may have experienced a lagged response to any sea-level rise. This may be one explanation for the difference in timing of any fluctuations between this and other records. The difference in the rate of salt-marsh response to RSL change is an important consideration when resolving the spatial and temporal patterns of sea-level change.

All three previously published salt-marsh reconstructions (which in Figure 9 are plotted with 2σ errors, compared to the usually reported 1σ errors) record intervals in which sea level rose in the pre-industrial era. The oldest sea-level rise is dated in Iceland to ~AD 200 (Gehrels et al., 2006a), in

New Jersey from ~AD 230 to AD 730 with sea-level rising at 0.6 mm yr^{-1} (Kemp et al., 2013), and in North Carolina between ~AD 950 to AD 1375 when the rate of RSL rise was 0.5 mm yr^{-1} (Kemp et al., 2011; Kemp et al., 2013). The North Carolina and New Jersey records have a greater number of radiocarbon dates than the older part of the Icelandic reconstruction, which is chronological anchored by two tephras. The RSL changes in both the North Carolina and New Jersey records differ in timing, but both rates exceed the modelled background rate of RSL fall in north west Scotland (~-0.4 mm yr^{-1}). If these were basin-wide signals, they should result in a positive tendency in the Scottish records, but this is not the case, suggesting they are local or regionally specific signals. Regional processes, including oceanographic forcing associated with changes in Atlantic Meridional Overturning Circulation (AMOC) and Gulf Stream strength, are particularly important in the western Atlantic (Kopp et al., 2010; Long et al., 2014; Vazquez et al., 1990) where salt marshes are a valuable archive for recording these processes on multi-decadal to centennial timescales (Long et al., 2014).

6.3 Implications for understanding the driving mechanisms of sea-level change during the last two millennia

An issue common to many palaeoenvironmental studies is upscaling from the local to the regional and/or global and seeking comparisons or correlations between different time series. In reality, the quality, number and spatial distribution of sites is often insufficient to do so. This danger is all too apparent in this and other sea-level studies on the late Holocene. Indeed, we opened this paper by noting that there were only three other continuous salt-marsh records of RSL change from the North Atlantic and that these were not the same. Notwithstanding the small number and contradictory signals, it is common to seek driving mechanisms for parts of, and in some instances, all of the patterns observed.

We acknowledge that the records have important limitations that restrict our ability to infer causal mechanisms from it. Firstly, the age and altitude errors are large; the data are generated from a macrotidal environment which means that the 1σ vertical precision of the reconstructions is typically ±0.4 m (2σ error ±0.8 m). Secondly, the accumulation rate on the marshes is low and this limits the resolution of the microfossil data. Thirdly, there are some diatom taxa present in the contemporary assemblages that are lacking in the fossil record. And finally, some of the radiocarbon dates are either from mixed sedimentary units (though these samples are excluded from the final reconstruction) or uncertain because of potential contamination.

The problems do not prevent us being able to draw four valuable conclusions from this study. Firstly, we are confident, from the lithology, biostratigraphy and age-depth models at the two field sites that the last two thousand years have been characterised by a long-term, gradual fall in RSL that was associated with a general pattern of marsh progradation (albeit one that was briefly interrupted at Loch Laxford). The sea-level tendency has been negative for the vast majority of time considered. This is wholly compatible with what is understood about the long-term GIA trend in Scotland (Bradley et al., 2011) and also suggests that the net contribution of the ice sheets to ocean volume over the last 2000 years may have been small. Secondly, whilst the uncertainties in the age and elevation of the sea-level data do not preclude the possibility that brief changes in the rate of sea-level change took place, the biostratigraphy points to only one interval in which a switch from the negative to a positive sea-level tendency occurred at both sites. This switch, dated to the AD 1940-1950s, is not associated with any sea-level change in the Aberdeen tide gauge, located on the North Sea coast of east Scotland and is, therefore restricted in its regional expression. We note the correlation between the timing of this change and an abrupt and sustained increase in fjord bottom water temperatures in Loch Sunart (200 km south of Loch Laxford) (Cage and Austin, 2010), as well as by a change in North Atlantic Oscillation (NAO) mode and a correlation with increased winter wave heights offshore of northwest Scotland (Allan et al., 2009). It is too soon to say with confidence whether this change in sea-level tendency is recorded elsewhere in Scotland but the coincidence in timing invites the hypothesis that these events may be linked.

The third conclusion is that, as indicated previously by the Aberdeen tide gauge, there is no evidence in the Scottish salt-marsh records for a significant acceleration in late 19th or early 20th century sea level. The slight acceleration indicated by the tide-gauge data is too small to be recorded in the salt marsh records. The lack of a strong post-industrialisation sea-level rise in northwest Scotland contrasts the strong signal in the western Atlantic basin, adding weight to the arguments of Long et al. (2014) that there are significant differences in the RSL histories between the North American and European coastlines over what we now understand to be several millennia, as opposed to a few centuries.

The fourth conclusion is that trends of sea-level change in this basin cannot be summarised by a single record from any single site. Indeed, the kind of variability that is emerging between this and other studies is precisely what one would expect, based upon understanding of the overlapping and often complex spatial and temporal patterns of sea-level variability caused by the dynamic interaction of atmosphere-ocean-cryosphere processes that operate over a variety of timescales.

Finally, we note that detection thresholds are sensitive to a range of parameters including the length of the record, the range of sea-level anomaly spanned by the network of records, and number and spread of the records. Increasing any of these parameters reduces the detection threshold (Kopp et al., 2010). As shown with tide-gauge records, detecting regional drivers of RSL change with synchronous timing requires a comprehensive network of long records (Kopp et al., 2010). This is particularly important with more complex salt-marsh RSL records where each record is not only a result of regional RSL change but also local site-specific processes (Barlow et al., 2013; Gehrels et al., 2004; Kirwan and Temmerman, 2009). Realistically, therefore, it is currently not possible, on the basis of the handful of available millennial-scale records, to reject the hypothesis that the differences in the tendencies of RSL change are not simply a consequence of regional to local processes.

7 Conclusions

By developing a multi-faceted approach to RSL reconstruction, we are able to present the first millennial-length continuous records of late Holocene RSL change from the eastern North Atlantic, and, uniquely, from an uplifting coastline. Multiple records allow us to develop confidence of regional RSL coherence away from site-specific noise. In developing these records we highlight methodological issues such as noise in RSL reconstruction as a consequence of the transfer function and variations in species assemblages. By assessing changes in tendency we are able to test modes of North Atlantic sea-level change independent of the complications of GIA correction. Our records suggest there have been no increases in the rate of RSL rise from ~AD 200-1940 greater than 0.4 mm yr^{-1} (the modelled background rate of late Holocene RSL fall in north west Scotland). We cannot reject the hypotheses of a 20th century sea-level acceleration, but it appears muted and later than recorded from the western North Atlantic. This may be suggestive of spatial differences in the drivers of RSL change. Assessing multi-centennial to millennial-scale drivers of RSL change requires a greater number of continuous, millennial-length, precise RSL reconstructions from both sides of the North Atlantic.

Acknowledgments

Funding for this work was provided by UK Natural Environment Research Council grant “North Atlantic sea-level change and climate in the last 500 years” (NE/G004757/1). Radiocarbon dating support comes from the Natural Environment Research Council Radiocarbon Facility (NRCF010001), grants #1490.0810, 1566.0511, 1604.0112, 1650.0612. We thank Jack Allen, Matthew Brain, Ben Cullen and Tim Dowson for their assistance in the field and Martin West and Amanda Hayton in the Geography Department at Durham University for preparation and analysis of the gamma and ICP-MS samples. The Reay Forest Estate, Kinloch Estate and Scottish Natural Heritage provided access to the salt marshes at Loch Laxford and Kyle of Tongue. We thank Ian Shennan for his thoughts on Scottish sea levels and inspiration for Figure 8, Andy Kemp for making his datasets available, Maarten Blaauw for Bacon advice, Sarah Bradley for providing the GIA model estimates and Phil Woodworth for the composite Aberdeen tide-gauge record. We thank David Kennedy and an anonymous reviewer who made helpful and constructive observations that improved the paper. This paper has benefited from discussions with members of PALSEA2 (an INQUA International Focus Group and a PAGES working group) and is a contribution to that program and to IGCP Project 588 "Preparing for coastal change: A detailed process-response framework for coastal change at different timescales".

References

Allan, R., Tett, S., Alexander, L., 2009. Fluctuations in autumn–winter severe storms over the British Isles: 1920 to present. Int. J. Climatol. 29, 357-371.
Appleby, P.G., Oldfield, F., 1983. The assessment of 210-Pb data from sites with varying sediment accumulation rates. Hydrobiologia 103, 29-35.
Baeteman, C., Waller, M., Kiden, P., 2011. Reconstructing middle to late Holocene sea-level change: A methodological review with particular reference to 'A new Holocene sea-level curve for the southern North Sea' presented by K.-E. Behre. Boreas 40, 557-572.
Balesdent, J., 1987. The turnover of soil organic fractions estimated by radiocarbon dating. Science of The Total Environment 62, 405-408.
Barlow, N.L.M., Shennan, I., Long, A.J., Gehrels, W.R., Saher, M.H., Woodroffe, S.A., Hillier, C., 2013. Salt marshes as geological tide gauges. Global and Planetary Change 106, 90-110.
Bates, C.R., Moore, C.G., Harries, D.B., Austin, W., Mair, J., 2004. Broad scale mapping of sublittoral habitats in Loch Laxford, Scotland., Scottish Natural Heritage Commissioned Report No. 004 (ROAME No. F01AA401A).
Birks, H.J.B., 1995. Quantitative palaeoenvironmental reconstructions, In: Maddy, D., Brew, J.S. (Eds.), Statistical modelling of Quaternary Science data. Quaternary Research Association., Cambridge, pp. 161-254.
Blaauw, M., Christen, A.J., 2011. Flexible Paleoclimate Age-Depth Models Using an Autoregressive Gamma Process. Bayesian Analysis 6, 457-474.
Bradley, S.L., Milne, G.A., Shennan, I., Edwards, R., 2011. An improved glacial isostatic adjustment model for the British Isles. Journal of Quaternary Science 26, 541-552.
Brain, M.J., Long, A.J., Woodroffe, S.A., Petley, D.N., Milledge, D.G., Parnell, A.C., 2012. Modelling the effects of sediment compaction on salt marsh reconstructions of recent sea-level rise. Earth and Planetary Science Letters 345, 180-193.
Bronk Ramsey, C., 2001. Development of the radiocarbon calibration program OxCal. Radiocarbon 43, 355-363.
Cage, A., Austin, W.E., 2010. Marine climate variability during the last millennium: The Loch Sunart record, Scotland, UK. Quaternary Science Reviews 29, 1633-1647.
Cronin, T.M., 2012. Rapid sea-level rise. Quaternary Science Reviews 56, 11-30.
Cullen, B.J., 2013. Decompacting a Late Holocene sea-level record from Loch Laxford, northwest Scotland., Masters thesis, Durham University.
Cundy, A.B., Croudace, I.W., 1995. Physical and chemical associations of radionuclides and trace metals in estuarine sediments: an example from Poole Harbour, southern England. Journal of Environmental Radioactivity 29, 191-211.
Cundy, A.B., Croudace, I.W., Thomson, J., Lewis, J.T., 1997. Reliability of salt marshes as "geochemical recorders" of pollution input : a case study from contrasting estuaries in southern England. Environmental Science and Technology 31, 1093-1101.
Dawson, S., Smith, D.E., Jordan, J., Dawson, A.G., 2004. Late Holocene coastal sand movements in the Outer Hebrides, N.W. Scotland. Marine Geology 210, 281-306.
Donnelly, J.P., 2006. A revised late Holocene sea-level record for northern Massachusetts, USA. Journal of Coastal Research 22, 1051-1061.
Donnelly, J.P., Cleary, P., Newby, P., Ettinger, R., 2004. Coupling instrumental and geological records of sea-level change: Evidence from southern New England of an increase in the rate of sea-level rise in the late 19th century. Geophysical Research Letters 31.
Edwards, R.J., 2001. Mid- to Late Holocene relative sea-level change in Poole Harbour, southern England. Journal of Quaternary Science 16, 221-235.
Engelhart, S.E., Horton, B.P., 2012. Holocene sea level database for the Atlantic coast of the United States. Quaternary Science Reviews 54, 12-25.

Fairbridge, R.W., 1992. Holocene marine coastal evolution of the United States, In: Fletcher, C.H., Wehmiller, J.F. (Eds.), Quaternary Coasts of the United States. Society of Sedimentary Geology, Special Publication 48, pp. 9-20.
Fatela, F., Taborda, R., 2002. Confidence limits of species proportions in microfossil assemblages. Marine Micropaleontology 45, 169-174.
Fletcher, C.H.I.I.I., Pizzulo, J.E., John, S., van Pelt, J.E., 1993. Sea-Level Rise Acceleration and the Drowning of the Delaware Bay Coast at 1.8ka. Geology 21, 121-124.
Gehrels, W.R., 1999. Middle and late holocene sea-level changes in Eastern Maine reconstructed from foraminiferal saltmarsh stratigraphy and AMS C-14 dates on basal peat. Quaternary Research 52, 350-359.
Gehrels, W.R., Belknap, D.F., Black, S., Newnham, R.M., 2002. Rapid sea-level rise in the Gulf of Maine, USA, since AD 1800. Holocene 12, 383-389.
Gehrels, W.R., Marshall, W.A., Gehrels, M.J., Larsen, G., Kirby, J.R., Eiriksson, J., Heinemeier, J., Shimmield, T., 2006a. Rapid sea-level rise in the North Atlantic Ocean since the first half of the nineteenth century. Holocene 16, 949-965.
Gehrels, W.R., Milne, G.A., Kirby, J.R., Patterson, R.T., Belknap, D.F., 2004. Late Holocene sea-level changes and isostatic crustal movements in Atlantic Canada. Quaternary International 120, 79-89.
Gehrels, W.R., Szkornik, K., Bartholdy, J., Kirby, J.R., Bradley, S.L., Marshall, W.A., Heinemeier, J., Pedersen, J.B.T., 2006b. Late Holocene sea-level changes and isostasy in western Denmark. Quaternary Research 66, 288-302.
González, J.L., Törnqvist, T.E., 2009. A new Late Holocene sea-level record from the Mississippi Delta: evidence for a climate/sea level connection? Quaternary Science Reviews 28, 1737-1749.
Grinsted, A., Jevrejeva, S., Moore, J.C., 2011. Comment on the subsidence adjustment applied to the Kemp et al. proxy of North Carolina relative sea level. Proceedings of the National Academy of Sciences 108, E781-E782.
Horton, B.P., Edwards, R.J., 2005. The application of local and regional transfer functions to the reconstruction of Holocene sea levels, north Norfolk, England. Holocene 15, 216-228.
Johnston, G.S., 1989. Northern Highlands of Scotland. British Geological Survey.
Kemp, A.C., Horton, B.P., Donnelly, J.P., Mann, M.E., Vermeer, M., Rahmstorf, S., 2011. Climate related sea-level variations over the past two millennia. Proceedings of the National Academy of Sciences of the United States of America 108, 11017-11022.
Kemp, A.C., Horton, B.P., Vane, C.H., Bernhardt, C.E., Corbett, D.R., Engelhart, S.E., Anisfeld, S.C., Parnell, A.C., Cahill, N., 2013. Sea-level change during the last 2500 years in New Jersey, USA. Quaternary Science Reviews 81, 90-104.
Kirwan, M., Temmerman, S., 2009. Coastal marsh response to historical and future sea-level acceleration. Quaternary Science Reviews 28, 1801-1808.
Komarek, M., Ettler, V., Chrastny, V., Mihaljevic, M., 2008. Lead isotopes in environmental sciences: A review. Environment International 34, 562-577.
Kopp, R.E., 2013. Does the mid-Atlantic United States sea level acceleration hot spot reflect ocean dynamic variability? Geophysical Research Letters 40, 3981-3985.
Kopp, R.E., Mitrovica, J.X., Griffies, S.M., Yin, J., Hay, C.C., Stouffer, R.J., 2010. The impact of Greenland melt on local sea levels: a partially coupled analysis of dynamic and static equilibrium effects in idealized water-hosing experiments. Climatic change 103, 619-625.
Kylander, M.E., Weiss, D.J., Kober, B., 2009. Two high resolution terrestrial records of atmospheric Pb deposition from New Brunswick, Canada, and Loch Laxford, Scotland. Science of the Total Environment 407, 1644-1657.
Leorri, E., Cearreta, A., 2009. Recent sea-level changes in the southern Bay of Biscay: transfer function reconstructions from salt-marshes compared with instrumental data. Scientia Marina 73, 287-296.

Long, A.J., Barlow, N.L.M., Gehrels, W.R., Saher, M.H., Woodworth, P.L., Scaife, R.G., 2014. Contrasting records of sea-level change in the eastern and western North Atlantic during the last 300 years. Earth and Planetary Science Letters 388, 110-122.
Mitrovica, J.X., Gomez, N., Morrow, E., Hay, C., Latychev, K., Tamisiea, M.E., 2011. On the robustness of predictions of sea level fingerprints. Geophysical Journal International 187, 729-742.
Moore, P.D., Webb, J.A., Collinson, M.E., 1991. Pollen Analysis. Blackwell, London.
Palmer, A.J., Abbott, W.H., 1986. Diatoms as indicators of sea level change, In: Van de Plassche, O. (Ed.), Sea Level Research: A manual for the collection and evaluation of data. Geobooks, Norwich, pp. 457-488.
Reimer, P.J., Baillie, M.G.L., Bard, E., Bayliss, A., Beck, J.W., Blackwell, P.G., Ramsey, C.B., Buck, C.E., Burr, G.S., Edwards, R.L., Friedrich, M., Grootes, P.M., Guilderson, T.P., Hajdas, I., Heaton, T.J., Hogg, A.G., Hughen, K.A., Kaiser, K.F., Kromer, B., McCormac, F.G., Manning, S.W., Reimer, R.W., Richards, D.A., Southon, J.R., Talamo, S., Turney, C.S.M., van der Plicht, J., Weyhenmeye, C.E., 2009. IntCal09 and Marine09 radiocarbon age calibration curves, 0-50,000 years cal BP. Radiocarbon 51, 1111-1150.
Robbins, J.A., 1978. Geochemical and geophysical applications of radioactive lead isotopes, In: Nriago, J.P. (Ed.), Biogeochemistry of Lead, North Holland, Amsterdam, pp. 285-393.
Rossi, V., Horton, B.P., Corbett, D.R., Leorri, E., Perez-Belmonte, L., Douglas, B.C., 2011. The application of foraminifera to reconstruct the rate of 20th century sea level rise, Morbihan Golfe, Brittany, France. Quaternary Research 75, 24-35.
Sallenger, A.H., Jr., Doran, K.S., Howd, P.A., 2012. Hotspot of accelerated sea-level rise on the Atlantic coast of North America. Nature Climate Change 2, 884-888.
Shennan, I., Horton, B.P., 2002. Holocene land- and sea-level changes in Great Britain. Journal of Quaternary Science 17, 511-526.
Shennan, I., Milne, G., Bradley, S., 2012. Late Holocene vertical land motion and relative sea-level changes: lessons from the British Isles. Journal of Quaternary Science 27, 64-70.
Smith, D.E., Hunt, N., Firth, C.R., Jordan, J.T., Fretwell, P.T., Harman, M., Murdy, J., Orford, J.D., Burnside, N.G., 2012. Patterns of Holocene relative sea level change in the North of Britain and Ireland. Quaternary Science Reviews 54, 58-76.
Stuiver, M., Reimer, P.J., 1993. Extended 14C database and revised CALIB 3.0 radiocarbon calibration program. Radiocarbon 35, 215-230.
Szkornik, K., Gehrels, W.R., Kirby, J.R., 2006. Salt-marsh diatom distributions in Ho Bugt (western Denmark) and the development of a transfer function for reconstructing Holocene sea-level changes. Marine Geology 235, 137-150.
Szkornik, K., Gehrels, W.R., Murray, A.S., 2008. Aeolian sand movement and relative sea-level rise in Ho Bugt, western Denmark, during the 'Little Ice Age'. Holocene 18, 951-965.
Trouet, V., Scourse, J.D., Raible, C.C., 2012. North Atlantic storminess and Atlantic Meridional Overturning Circulation during the last Millennium: Reconciling contradictory proxy records of NAO variability. Global and Planetary Change 84–85, 48-55.
Turner, J., Innes, J.B., Simmons, I.G., 1989. Two pollen diagrams from the same site. New Phytologist 113, 409-416.
van de Plassche, O., 2000. North Atlantic climate-ocean variations and sea level in Long Island sound, Connecticut, since 500 cal yr AD. Quaternary Research 53, 89-97.
Vazquez, J., Zlotnicki, V., Fu, L.-L., 1990. Sea level variabilities in the Gulf Stream between Cape Hatteras and 50°W: A Geosat study. Journal of Geophysical Research: Oceans 95, 17957-17964.
Watcham, E.P., Shennan, I., Barlow, N.L.M., 2013. Scale considerations in using diatoms as indicators of sea level change: lessons from Alaska. Journal of Quaternary Science 28, 165-179.
Woodworth, P., Teferle, F., Bingley, R., Shennan, I., Williams, S., 2009. Trends in UK mean sea level revisited. Geophysical Journal International 176, 19-30.

	Loch Laxford	Portnancon, Loch Eriboll (Kyle of Tongue)
Highest astronomical tide (HAT)	2.99	3.00
Mean high water spring tide (MHWS)	2.40	2.42
Mean high water neap tide (MHWN)	1.00	1.22
Mean tide level (MTL)	0.25	0.30
Mean low water neap tide (MLWN)	-0.60	-0.58
Mean low water spring tide (MLWS)	-1.60	-1.88

Table 1 – Tidal values in meters relative to UK Ordnance Datum for Loch Laxford and Loch Eribol. Kyle of Tongue does not have detailed tidal measurements, though the tidal range is known to be similar to Loch Eriboll, and therefore the Loch Eriboll measurements are applied to Kyle of Tongue.

Sample code	Depth (cm)	Description	Dating method	Reported ^{14}C age(s) ± 1σ error
Loch Laxford: LA-3 (31 dates)				
SUERC-39456	1.25 ± 0.25	Humin bulk	Routine	106.55 ± 0.51 (% modern)
SUERC-39457	3.25 ± 0.25	Humin bulk	Routine	109.79 ± 0.51 (% modern)
SUERC-39458	5.25 ± 0.25	Humin bulk	Routine	101.70 ± 0.49 (% modern)
SUERC-39464 SUERC-39465 SUERC-39466	7.25 ± 0.25	Humin bulk	Routine Triplicate	191 ± 35 212 ± 35 197 ± 35
SUERC-39468 SUERC-39472 SUERC-39467	10.25 ± 0.25	Humin bulk	Routine Triplicate	187 ± 35 203 ± 35 162 ± 35
SUERC-39473 SUERC-39474 SUERC-39475	13.25 ± 0.25	Humin bulk	Routine Triplicate	266 ± 35 300 ± 35 257 ± 35
SUERC-33514 SUERC-33515	15.25 ± 0.25	Humin-humic bulk	Routine	327 ± 35 (humin) 338 ± 37 (humic)
SUERC-39480 SUERC-39481 SUERC-39476	16.25 ± 0.25	Humin bulk	Routine Triplicate	233 ± 35 237 ± 35 263 ± 35
SUERC-39482 SUERC-39483 SUERC-39484	17.25 ± 0.25	Humin bulk	Routine Triplicate	476 ± 35 443 ± 35 414 ± 35
SUERC-44998	21.25 ± 0.25	Humin bulk	Routine	549 ± 37
SUERC-44999	26.25 ± 0.25	Humin bulk	Routine	859 ± 37
SUERC-32493 SUERC-32496	30.25 ± 0.25	Humin-humic bulk	Routine	1097 ± 35 (humin) 846 ± 37 (humic)
SUERC-45000	36.25 ± 0.25	Humin bulk	Routine	880 ± 35
SUERC-39487	40.25 ± 0.25	Humin bulk	Routine	1434 ± 35
SUERC-32494 SUERC-32497	45.25 ± 0.25	Humin-humic bulk	Routine	1654 ± 37 (humin) 1176 ± 37 (humic)
SUERC-45001	53.25 ± 0.25	Humin bulk	Routine	1347 ± 37
SUERC-32495 SUERC-32498	60.25 ± 0.25	Humin-humic bulk	Routine	1717 ± 37 (humin) 1314 ± 37 (humic)
Loch Laxford: LA-6 (33 dates)				
SUERC-35801 SUERC-35802 SUERC-35803	4.5 ± 0.5	Humin bulk	HP Triplicate	108.68 ± 0.25 (% modern) 108.82 ± 0.30 (% modern) 108.28 ± 0.27 (% modern)
SUERC-35804 SUERC-35805 SUERC-35806	8.5 ± 0.5	Humin bulk	HP Triplicate	119.45 ± 0.32 (% modern) 118.96 ± 0.32 (% modern) 118.97 ± 0.29 (% modern)
SUERC-35807 SUERC-35811 SUERC-35812	12.5 ± 0.5	Humin bulk	HP Triplicate	106.40 ± 0.29 (% modern) 106.38 ± 0.29 (% modern) 106.76 ± 0.26 (% modern)
SUERC-35813 SUERC-35814 SUERC-35815	16.5 ± 0.5	Humin bulk	HP Triplicate	21 ± 20 92 ± 22 81 ± 22
SUERC-35816 SUERC-35817 SUERC-35821	20.5 ± 0.5	Humin bulk	HP Triplicate	264 ± 21 249 ± 20 232 ± 20

SUERC-35834 SUERC-35835 SUERC-35836	24.5 ± 0.5	Humin bulk	HP Triplicate	595 ± 21 606 ± 22 562 ± 21
SUERC-35837 SUERC-35841 SUERC-35842	28.5 ± 0.5	Humin bulk	HP Triplicate	683 ± 21 664 ± 21 683 ± 21
SUERC-35844 SUERC-35845 SUERC-35846	32.5 ± 0.5	Humin bulk	HP Triplicate	583 ± 21 581 ± 21 614 ± 21
SUERC-35847 SUERC-35851 SUERC-35852	36.5 ± 0.5	Humin bulk	HP Triplicate	610 ± 20 586 ± 22 592 ± 21
SUERC-35853 SUERC-35854 SUERC-35855	40.5 ± 0.5	Humin bulk	HP Triplicate	678 ± 21 658 ± 21 681 ± 20
SUERC-35856 SUERC-35857 SUERC-35861	44.5 ± 0.5	Humin bulk	HP Triplicate	878 ± 21 853 ± 19 865 ± 20
Kyle of Tongue: KT-3 (33 dates)				
SUERC-39302	2.5 ± 0.5	Plant macrofossils	Routine	116.81 ± 0.55 (% modern)
SUERC-39303	4.5 ± 0.5	Plant macrofossils	Routine	157.24 ± 0.71 (% modern)
SUERC-43535 SUERC-43537	5.25 ± 0.25	Plant macrofossils Humin bulk	HP	108 ± 17 105.48 ± 0.24 (% modern)
SUERC-43536 SUERC-43538	6.75 ± 0.25	Plant macrofossils Humin bulk	HP	52 ± 18 102.09 ± 0.23 (% modern)
SUERC-39540	8.5 ± 0.5	Plant macrofossils	HP	38 ± 35
SUERC-39502* SUERC-39503* SUERC-39504*	12.25 ± 0.25	Humin bulk	HP Triplicate	*100.71 ± 0.44 (% modern)* *100.96 ± 0.44 (% modern)* *101.58 ± 0.44 (% modern)*
SUERC-39505 SUERC-39506 SUERC-39510	16.25 ± 0.25	Humin bulk	HP Triplicate	27 ± 35 54 ± 35 36 ± 35
SUERC-39511* SUERC-39512* SUERC-39513*	20.25 ± 0.25	Humin bulk	HP Triplicate	*101.77 ± 0.44 (% modern)* *101.97 ± 0.44 (% modern)* *101.75 ± 0.44 (% modern)*
SUERC-45002	21.25 ± 0.25	Humin bulk	Routine	298 ± 37
SUERC-39519 SUERC-39520 SUERC-39521	24.25 ± 0.25	Humin bulk	HP Triplicate	441 ± 35 420 ± 35 439 ± 35
SUERC-45005	28.25 ± 0.25	Humin bulk	Routine	585 ± 35
SUERC-43539	32.25 ± 0.25	Humin bulk	HP	935 ± 18
SUERC-45006	36.25 ± 0.25	Humin bulk	Routine	880 ± 37
SUERC-43540	40.25 ± 0.25	Humin bulk	HP	1353 ± 18
SUERC-45007	44.25 ± 0.25	Humin bulk	Routine	1183 ± 35
SUERC-43541	50.25 ± 0.25	Humin bulk	HP	2065 ± 18
SUERC-39519 SUERC-39520 SUERC-39521	60.25 ± 0.25	Humin bulk	HP Triplicate	1686 ± 35 1689 ± 35 1682 ± 35
SUERC-43546	76.25 ± 0.25	Humin bulk	HP	2095 ± 20
SUERC-39525	86.25 ± 0.25	Humin bulk	HP	1745 ± 35

SUERC-39526 SUERC-39527			Triplicate	1743 ± 35 1724 ± 35

Table 2 – Radiocarbon dates from Loch Laxford (LA-3 and LA-6) and Kyle of Tongue (KT-3) used to develop the age models (as given in supplementary information). HP = high precision. * *Samples considered outliers and excluded from the age model.*

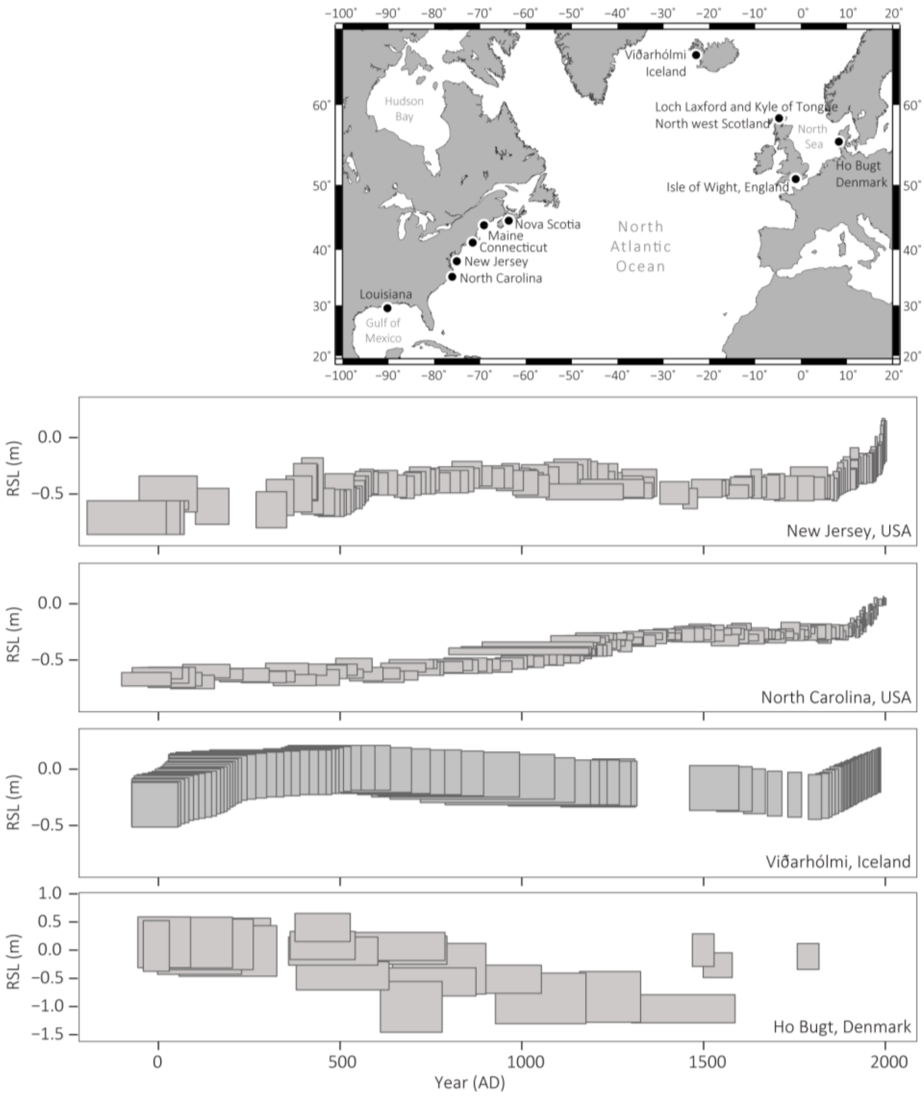

Figure 1 – Map of North Atlantic and key locations mentioned in the text. Graphs show 2000 year salt marsh based relative sea-level reconstructions from New Jersey and North Carolina, USA and Iceland; plus a basal/intercalated sea-level record from the eastern North Atlantic (Ho Bugt, western Denmark). All records have been detrended for background long-term RSL using values stated in the original papers: Iceland 0.65 mm yr^{-1} (Gehrels et al., 2006); New Jersey 1.4 mm yr^{-1} (Kemp et al., 2013); North Carolina 0.9 or 1.0 m yr^{-1} (Kemp et al., 2011). For Ho Bugt (Gehrels et al., 2006b; Szkornik et al., 2008) we assume a linear rate through the last 2000 years and detrend the record by 0.7 mm yr^{-1} (detailed in supplementary information). In all instances we only plot the samples which cover AD 0 to present, with 2σ age and 1σ attitude errors reported by the original authors. Note the different y-axis for the Ho Bugt record.

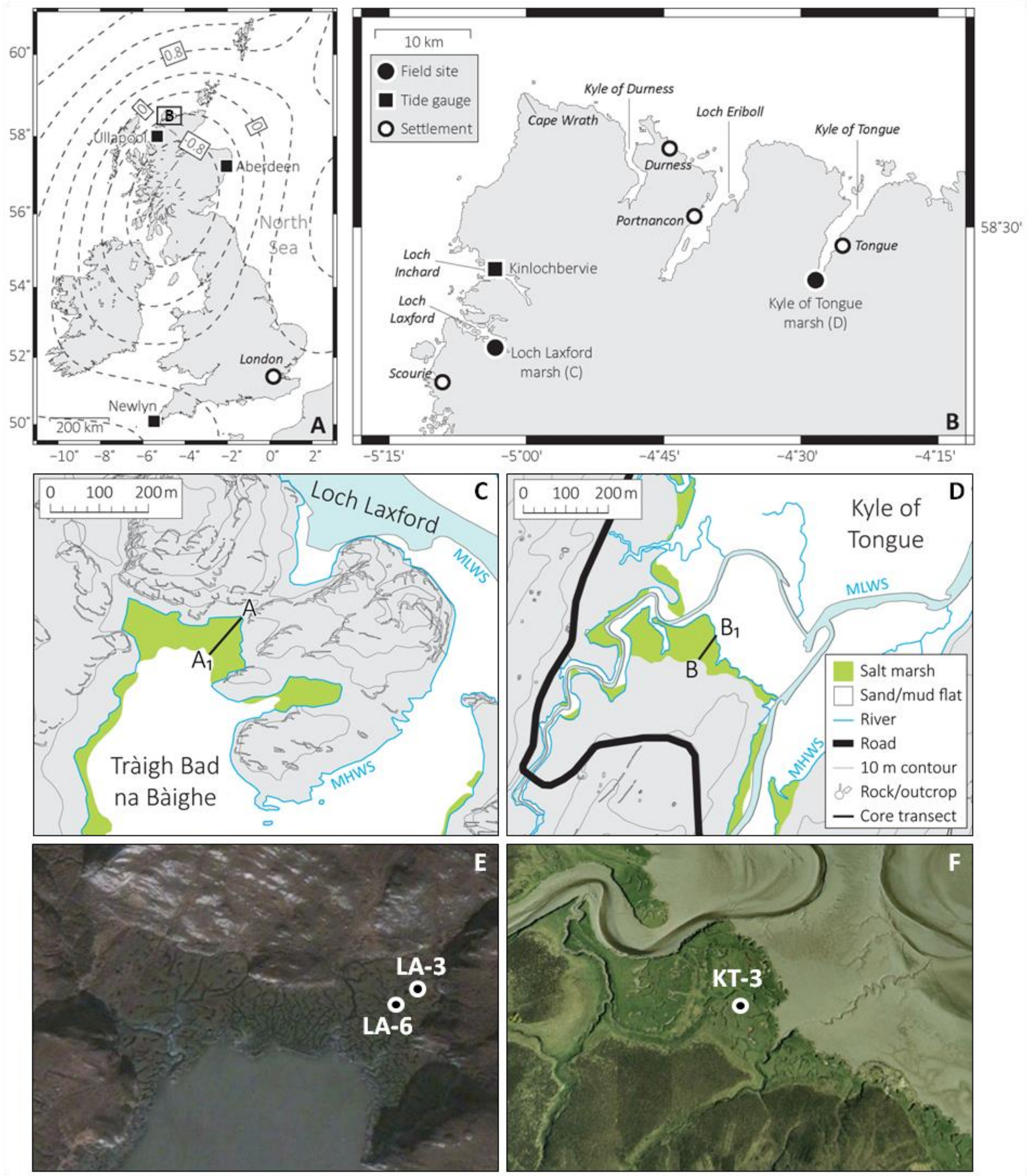

Figure 2 – Location of the field sites in north west Scotland. A: Map of the United Kingdom and Ireland showing the rates of long-term late Holocene RSL change (mm yr-1) (Bradley et al., 2011) and key tide gauge locations. B: Map of north west Scotland showing the location of the field sites. C and D: Maps of the Loch Laxford and Kyle of Tongue field sites respectively and the location of the transects in Figure 3. E and F: Google Earth images of the main part of the Loch Laxford and Kyle of Tongue marshes respectively with the sample core locations marked.

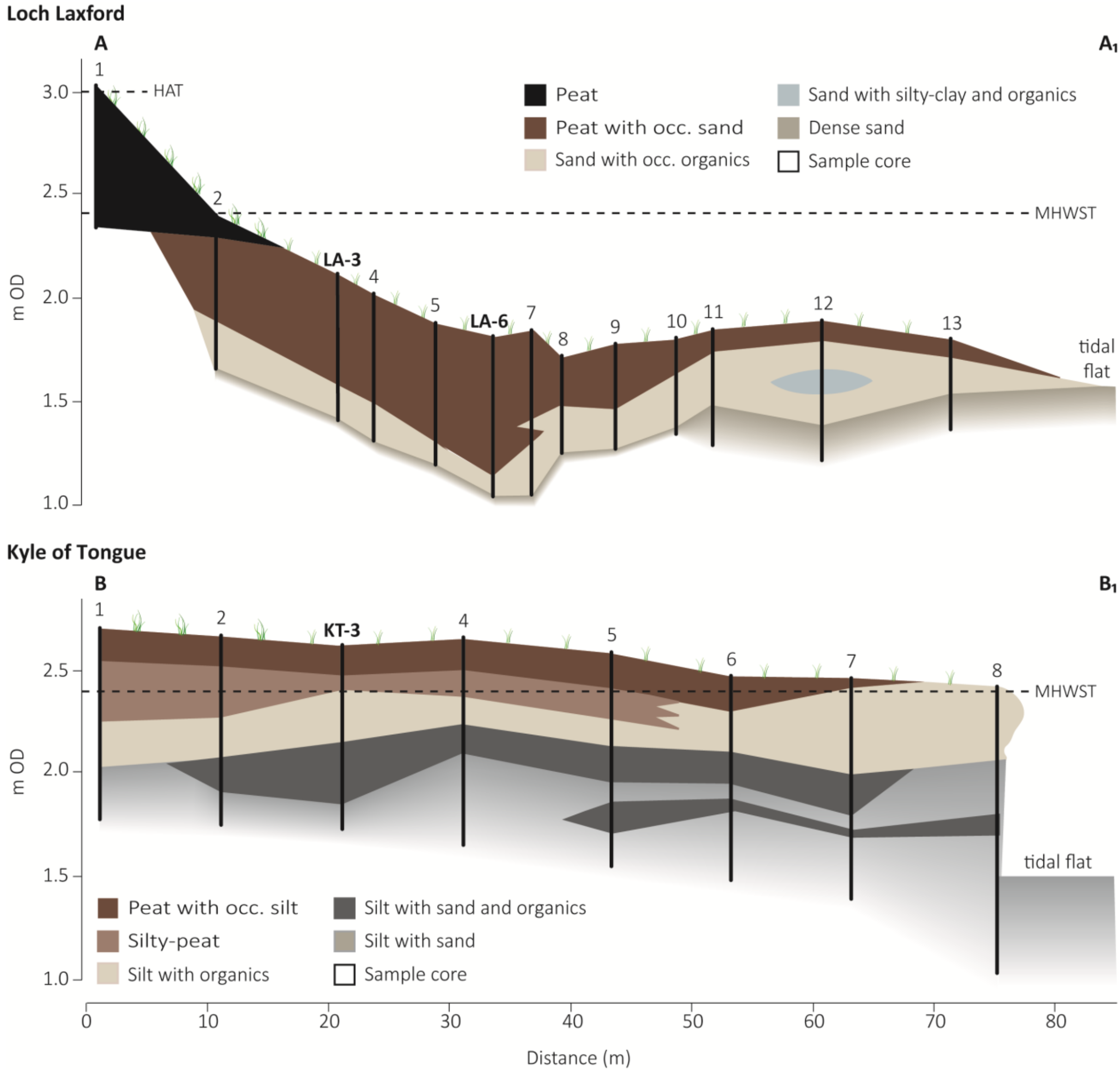

Figure 3 – Transect of cores and sediment lithology at Loch Laxford and Kyle of Tongue relative to Ordnance Datum (OD). The locations of the transects are shown on Figure 2.

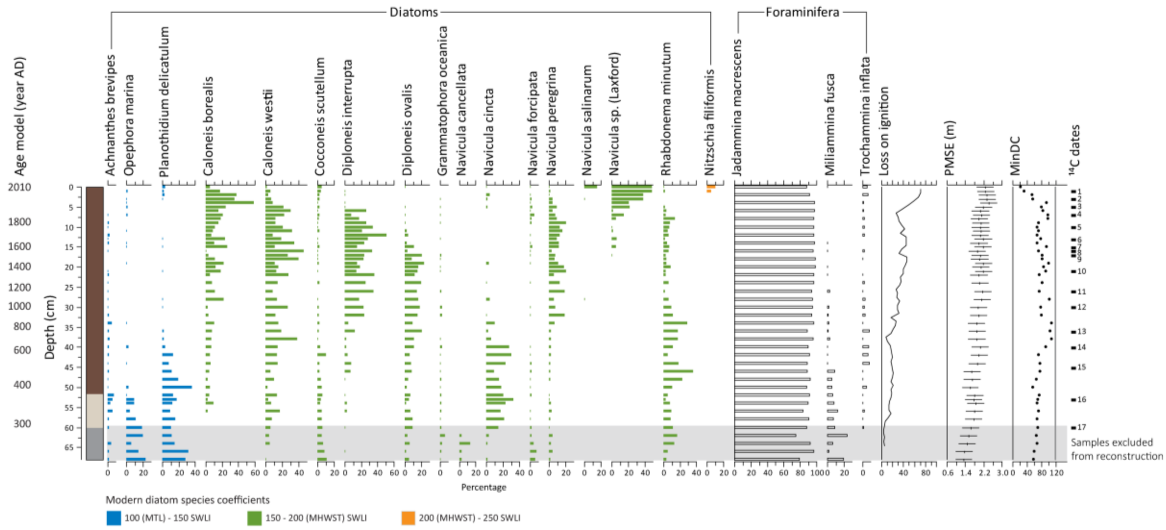

Figure 4 – Litho- and biostratigraphy at LA-3. Lithology colours as per the key in Figure 3. Diatoms shown for species greater than 5% of total valves counted and coloured and ordered according to modern diatom species coefficients (supplementary information Figure 3). MinDC values for each fossil sample are shown against the 20th percentile of the dissimilarity coefficients calculated between all modern samples (grey line). The LOI data comes from Cullen (2013). The grey boxed area shows the samples excluded from the RSL reconstruction in Figure 8 as detailed in the text.

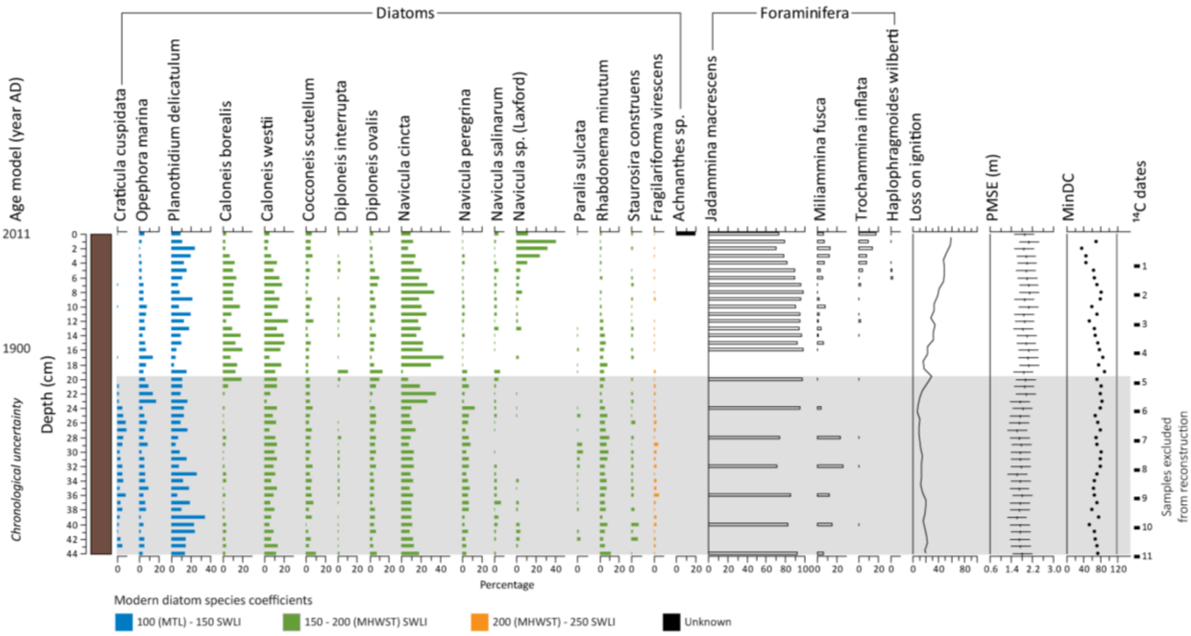

Figure 5 – Litho- and bio-stratigraphy at LA-6. Lithology colours as per the key in Figure 3. Diatoms shown for species greater than 5% of total valves counted and coloured and ordered according to modern diatom species coefficients (supplementary information Figure 3). MinDC values for each fossil sample are shown against the 20th percentile of the dissimilarity coefficients calculated between all modern samples (grey line). The grey boxed area shows the samples excluded from the RSL reconstruction in Figure 8 as detailed in the text.

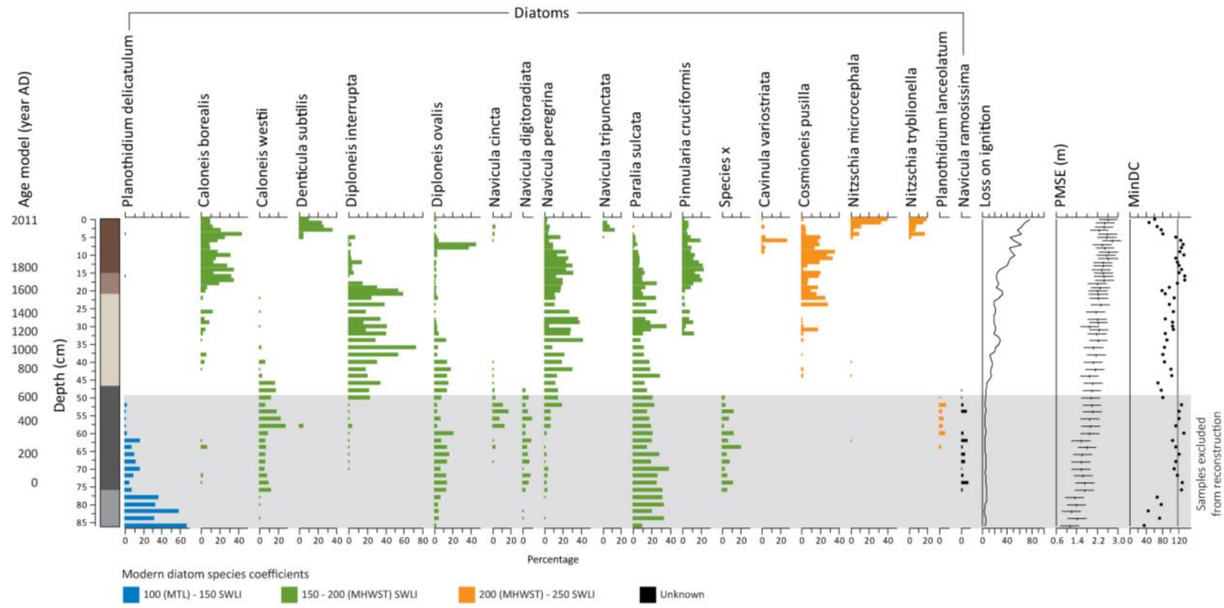

Figure 6 – Litho- and bio-stratigraphy at KT-3. Lithology colours as per the key in Figure 3. Diatoms shown for species greater than 5% of total valves counted and coloured and ordered according to modern diatom species coefficients (supplementary information Figure 3). MinDC values for each fossil sample are shown against the 20th percentile of the dissimilarity coefficients calculated between all modern samples (grey line). The grey boxed area shows the samples excluded from the RSL reconstruction in Figure 8 as detailed in the text.

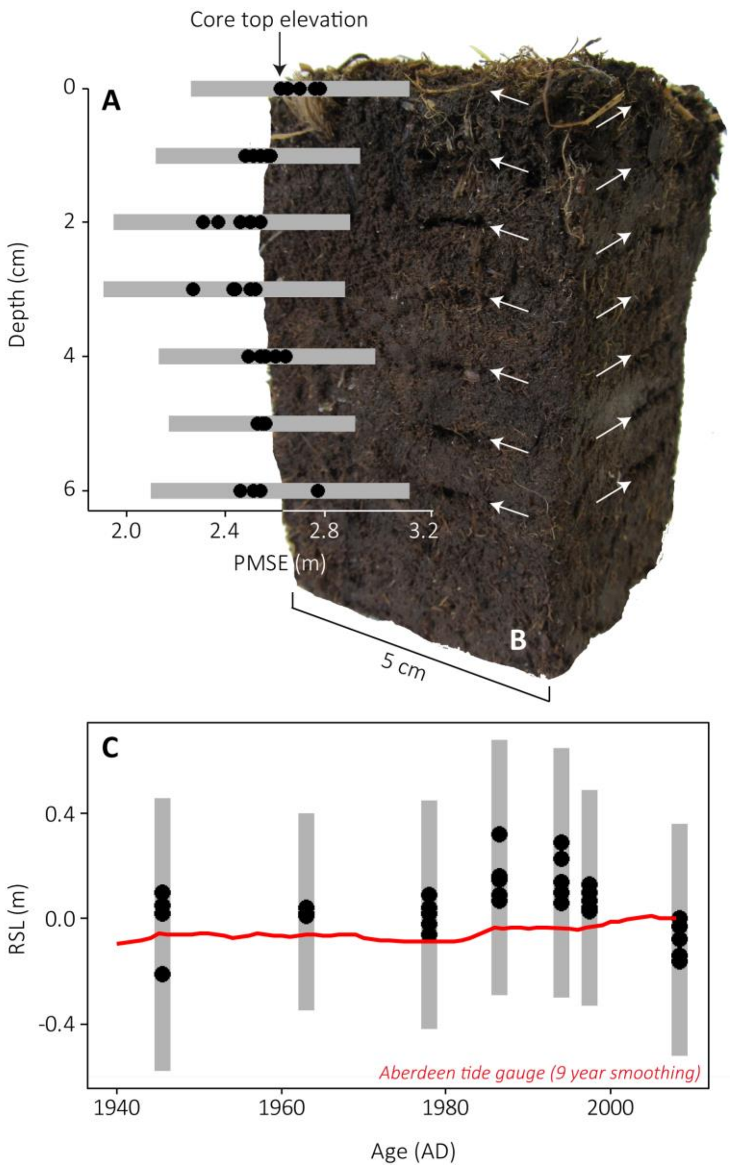

Figure 7 – A: Reconstructed palaeomarsh surface elevations (PMSE) of the top 6 cm of KT-3 and samples taken from the four sides of a proximal sediment block (shown in photo 'B' with the sampled depths of two of the faces marked by the white arrows) with associated overlapping 1σ error bars. The surveyed KT-3 core-top elevation is marked to check the transfer function results. C: The reconstructed elevations and associated errors from 'A' are converted to RSL, plotted against the KT-3 age model and compared to the Aberdeen tide gauge (with a 9-year moving average smoothing). Tide-gauge data are sourced from the Permanent Service for Mean Sea-level (http://www.psmsl.org/). The spread of the reconstructed elevation of the samples from each depth (the five black circles) demonstrates the noise associated with any RSL reconstruction.

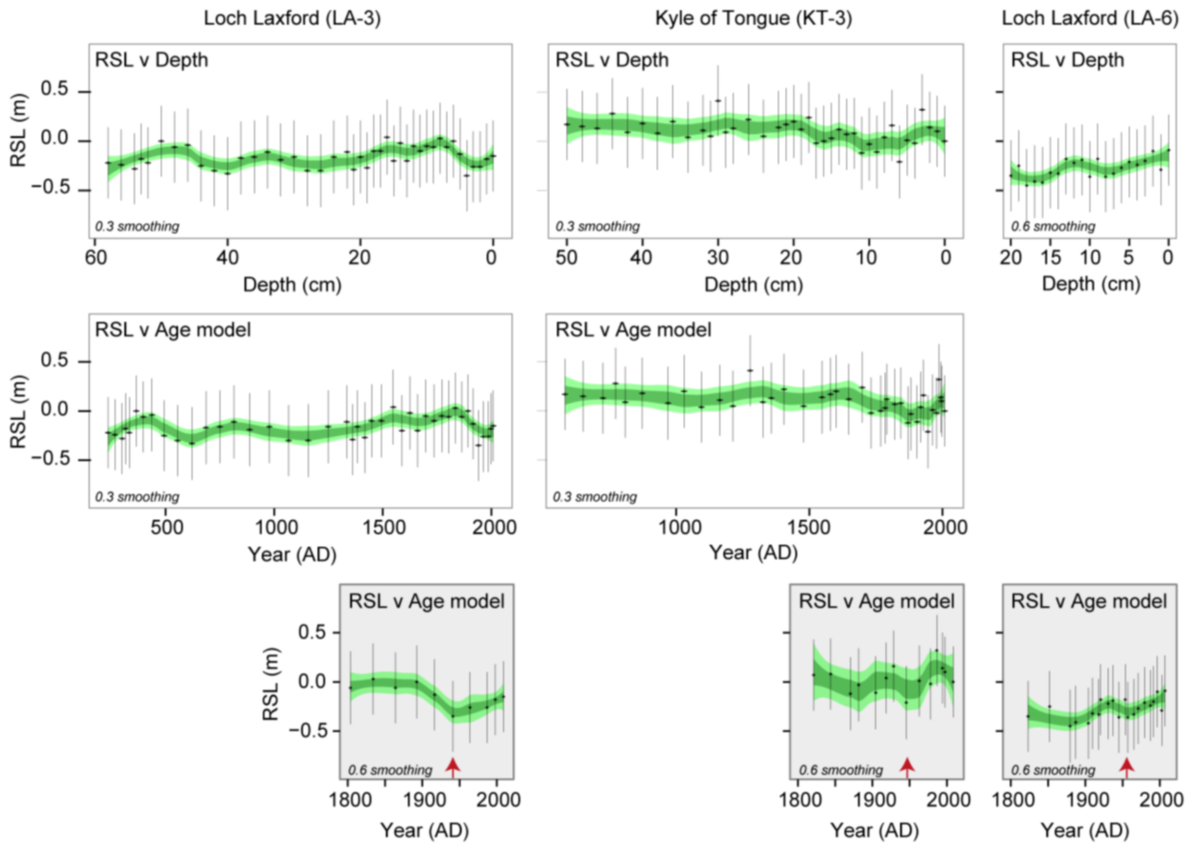

Figure 8 – Plots of relative sea level against depth (top row) and against age (bottom two rows) for the three cores: LA-3 and LA-6 from Loch Laxford and KT-3 from Kyle of Tongue with 1σ error bars. Dark green (68% SE) and light green (95% SE) band is a local polynomial regression fit with a smoothing function applied to test for multi-decadal changes in the sign of sea level. The bottom row (greyed boxes) shows the last 200 years of all three records and the smoothing function is doubled due to sampling resolution being every 1 cm in the top part of the cores. The red arrows mark the change in all three records from a negative to positive sea level at ~AD 1945-1955. Age errors are not shown for clarity; see Figure 9 for full age and altitudinal errors.

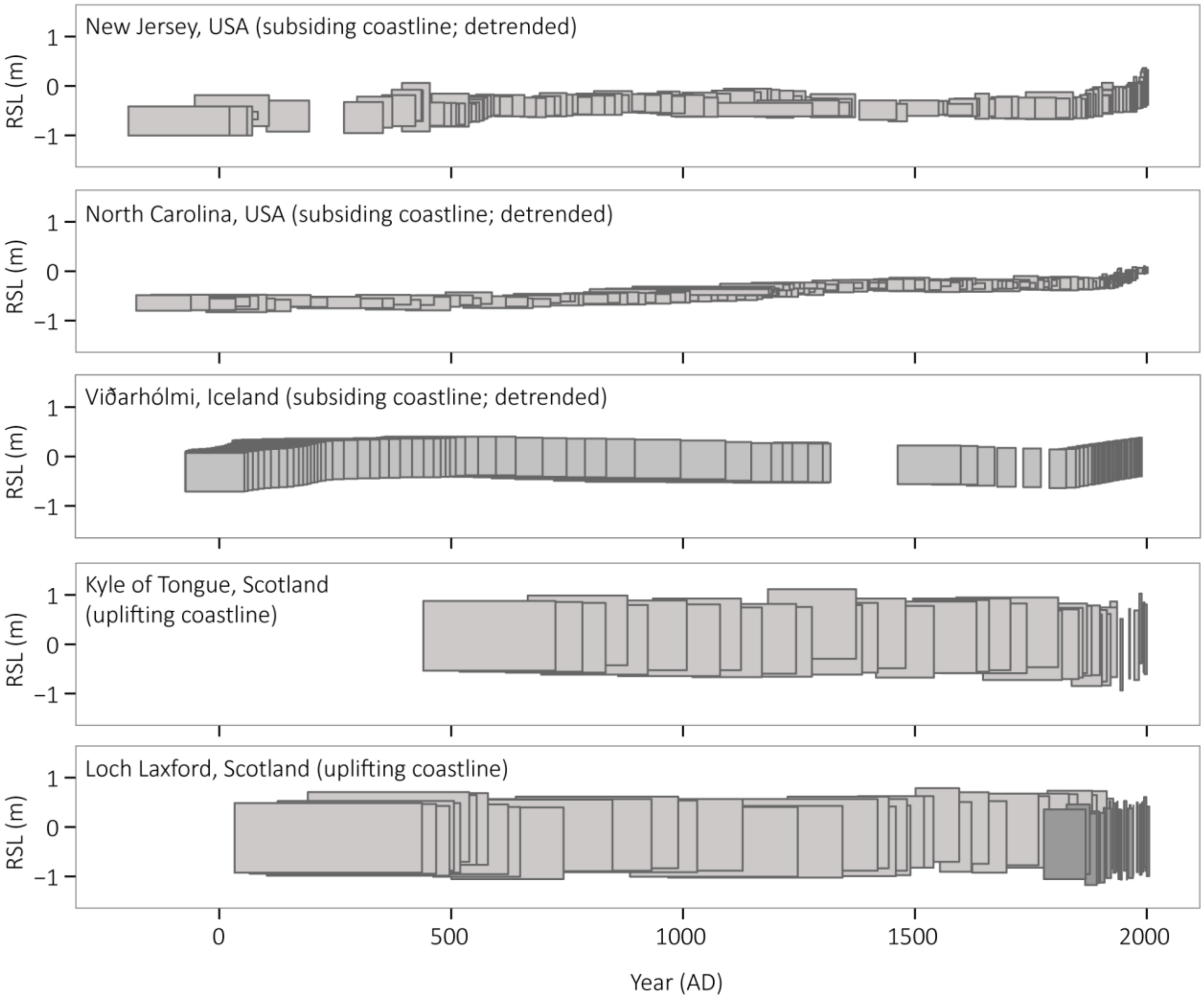

Figure 9 – All 2000 year continuous salt-marsh reconstructions from the North Atlantic plotted with 2σ age and altitudinal errors. Records from New Jersey (Kemp et al., 2013), North Carolina (Kemp et al., 2011) and Iceland (Gehrels et al., 2006) are detrended for background RSL rise as detailed in Figure 1. Scotland records are not detrended. Dark grey boxes in Loch Laxford reconstruction are LA-6 data points, with the longer LA-3 record shown by lighter grey boxes. The difference in the size of the vertical errors bars are primarily a consequence of the tidal range at each site (as discussed in Barlow et al., 2013).

Salt-marsh reconstructions of relative sea-level change in the North Atlantic during the last 2000 years

Barlow, N.L.M., Long, A.J., Saher, M.H., Gehrels, W.R., Garnett, M.H., Scaife, R.G.

Quaternary Science Reviews, 2014

Supplementary Information

Supplementary Figure 1	^{206}Pb/^{207}Pb profile for LA-3
Supplementary Figure 2	Scatterplot of the observed standardised water level index (SWLI) against the WA-PLS transfer function model predicted SWLI for the regional Scotland 'coastal transition' diatom training set for the second component from Barlow et al. (2012).
Supplementary Figure 3	Species coefficients for species >10% of valves counted in modern dataset based up the bootstrapped component 1 WA-PLS coefficients calculated in C2.
Supplementary Figure 4	Pollen profile from LA-6 (analyst Prof Rob Scaife)
Supplementary Figure 5	BACON age model for core LA-3
Supplementary Figure 6	BACON age model for core LA-6
Supplementary Figure 7	BACON age model for core KT-3
Supplementary Figure 8	Last 2000 years of sea level data from Ho Bugt, Denmark (Gehrels et al., 2006b; Szkornik et al., 2008). We assume a linear rate through the last 2000 years intercepting at the present day (zero on the y-axis), which produces an average rate of 0.7 mm yr^{-1}. We use this to detrend the data in Figure 1.

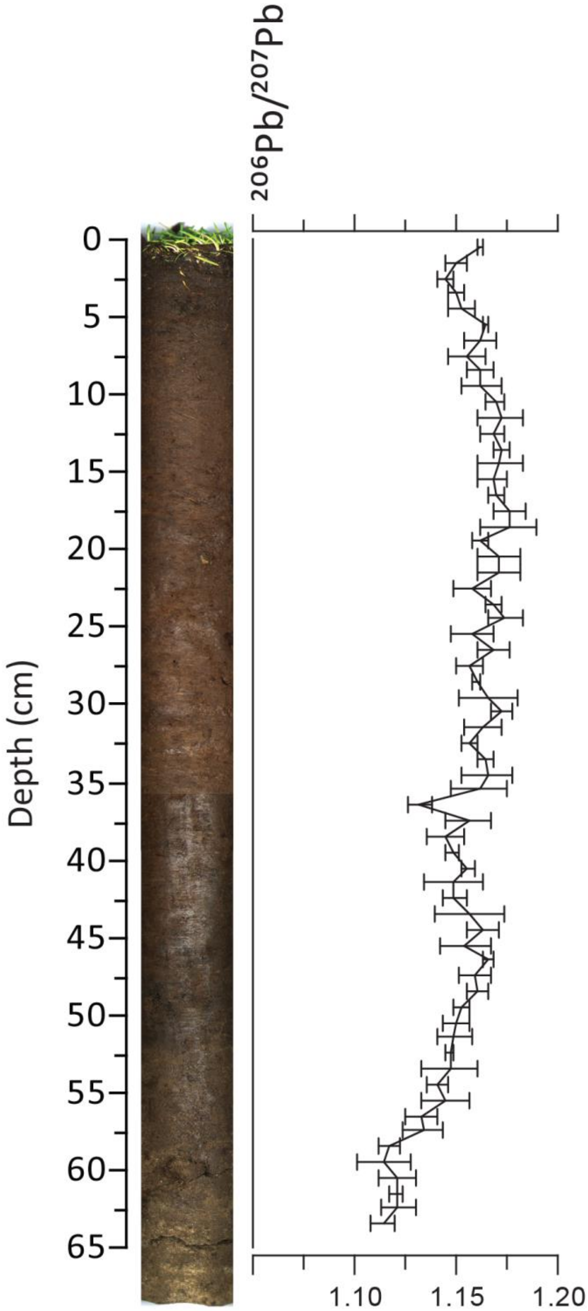

Supplementary Figure 1

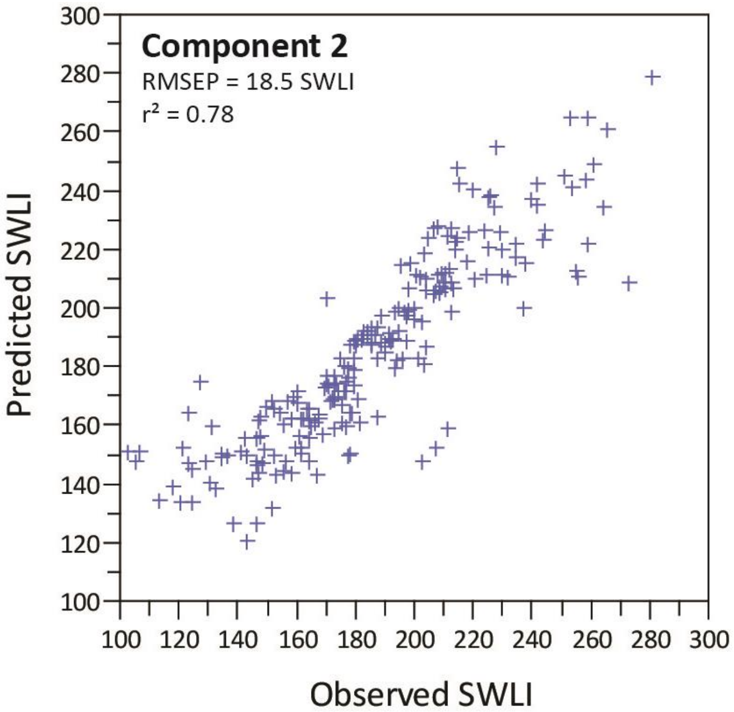

Supplementary Figure 2

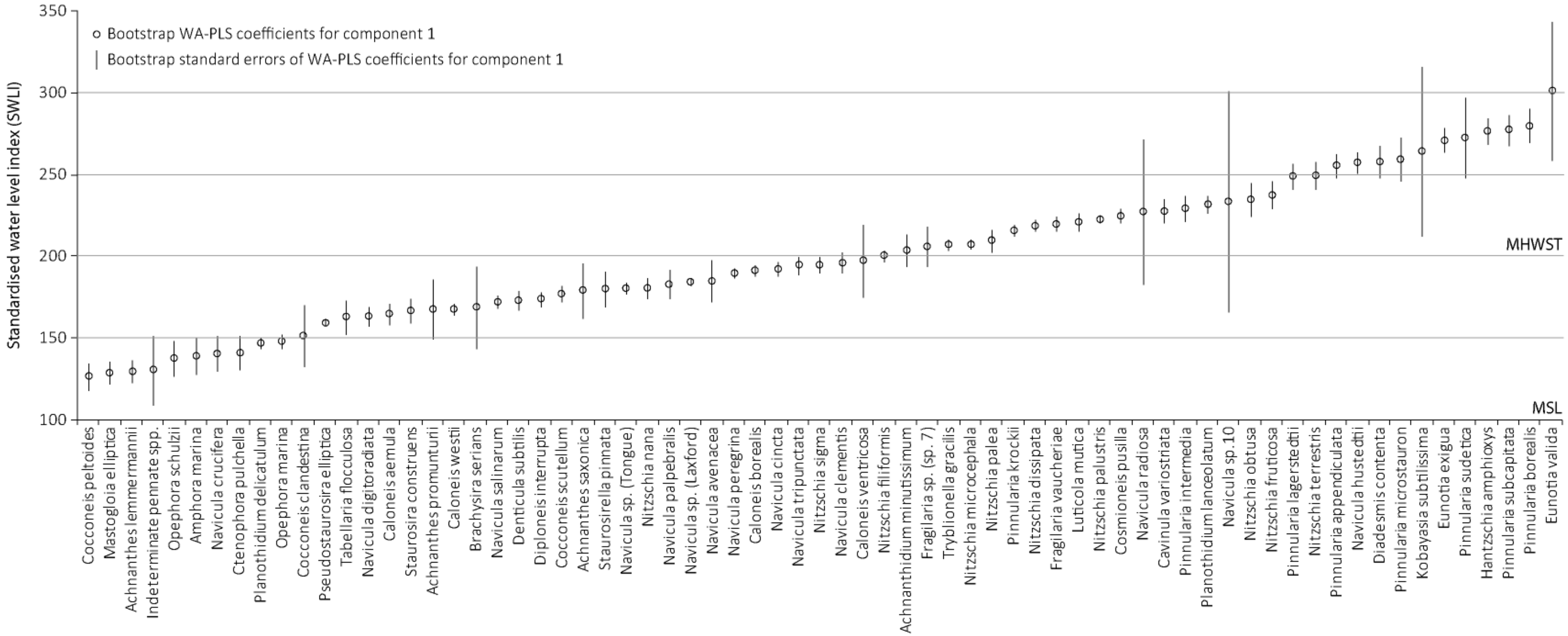

Supplementary Figure 3

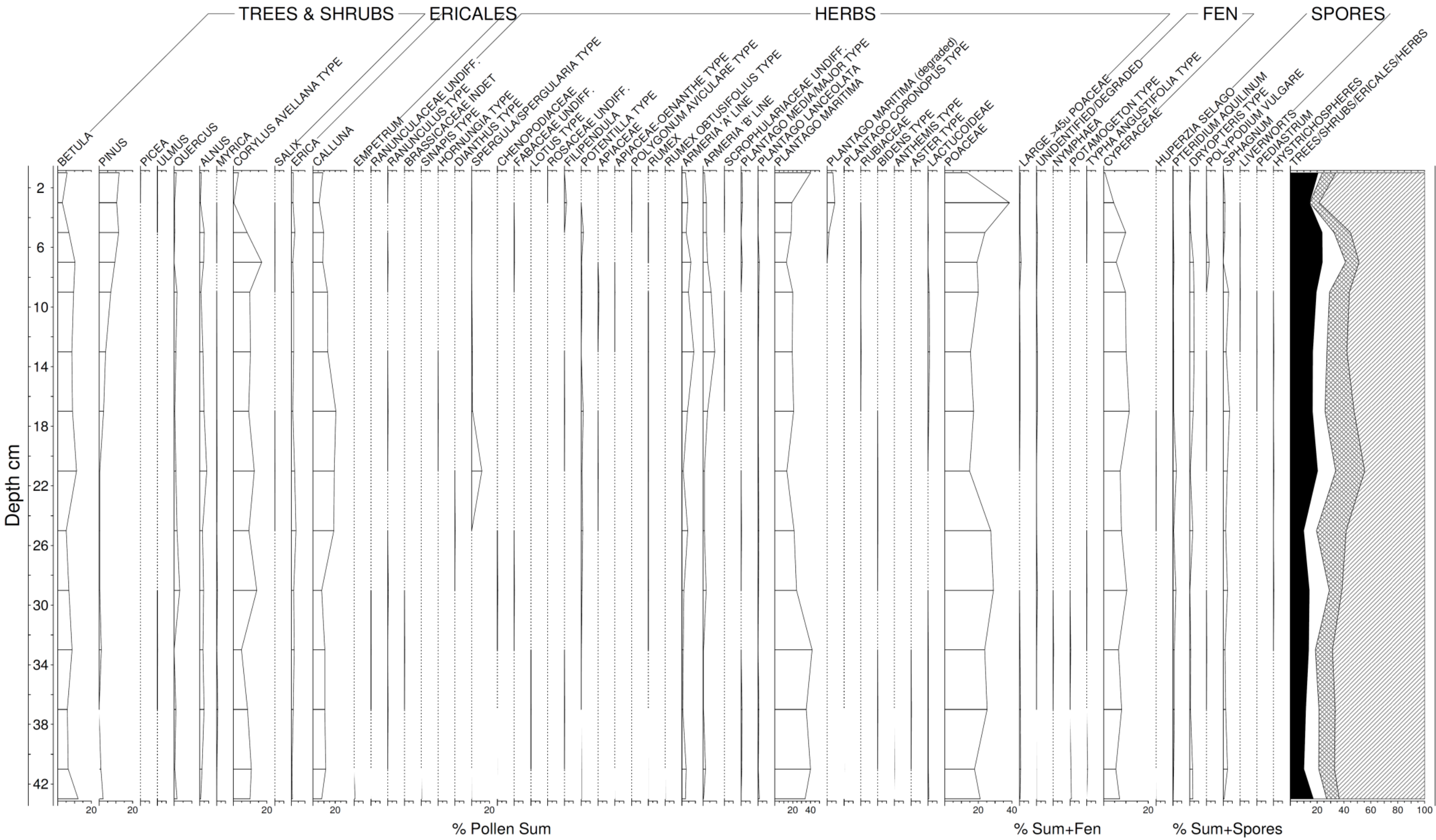

Supplementary Figure 4

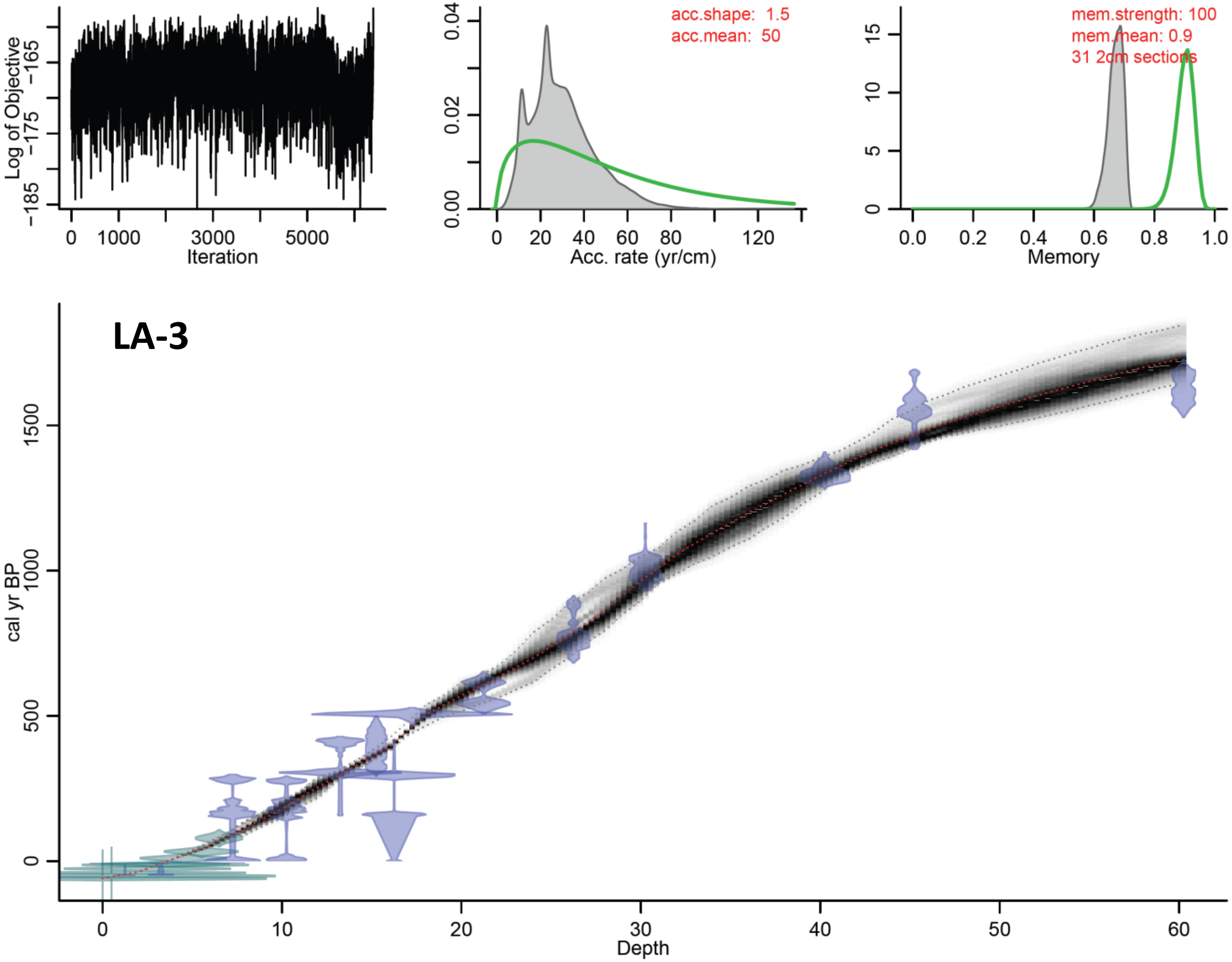

Supplementary Figure 5

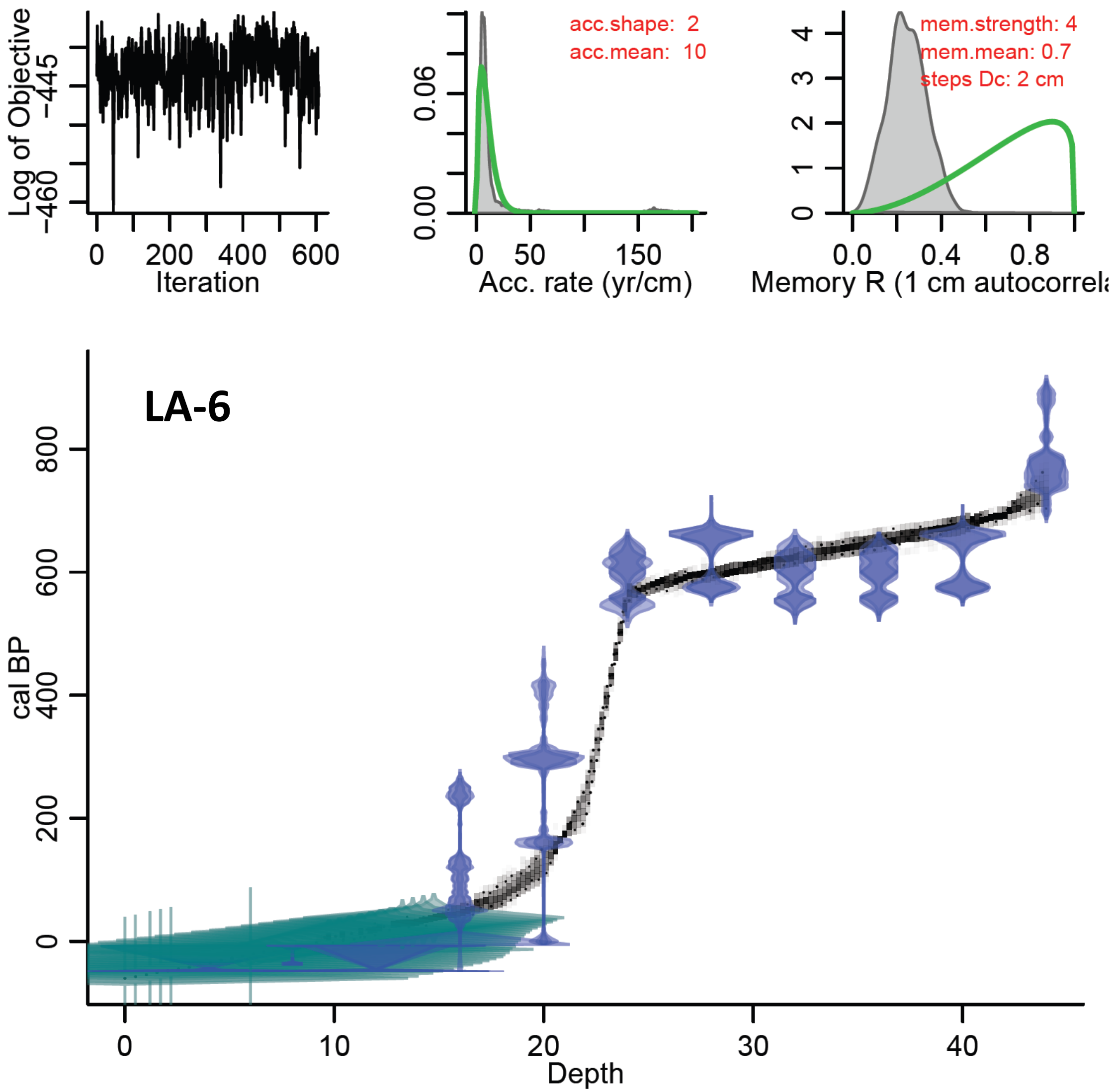

Supplementary Figure 6

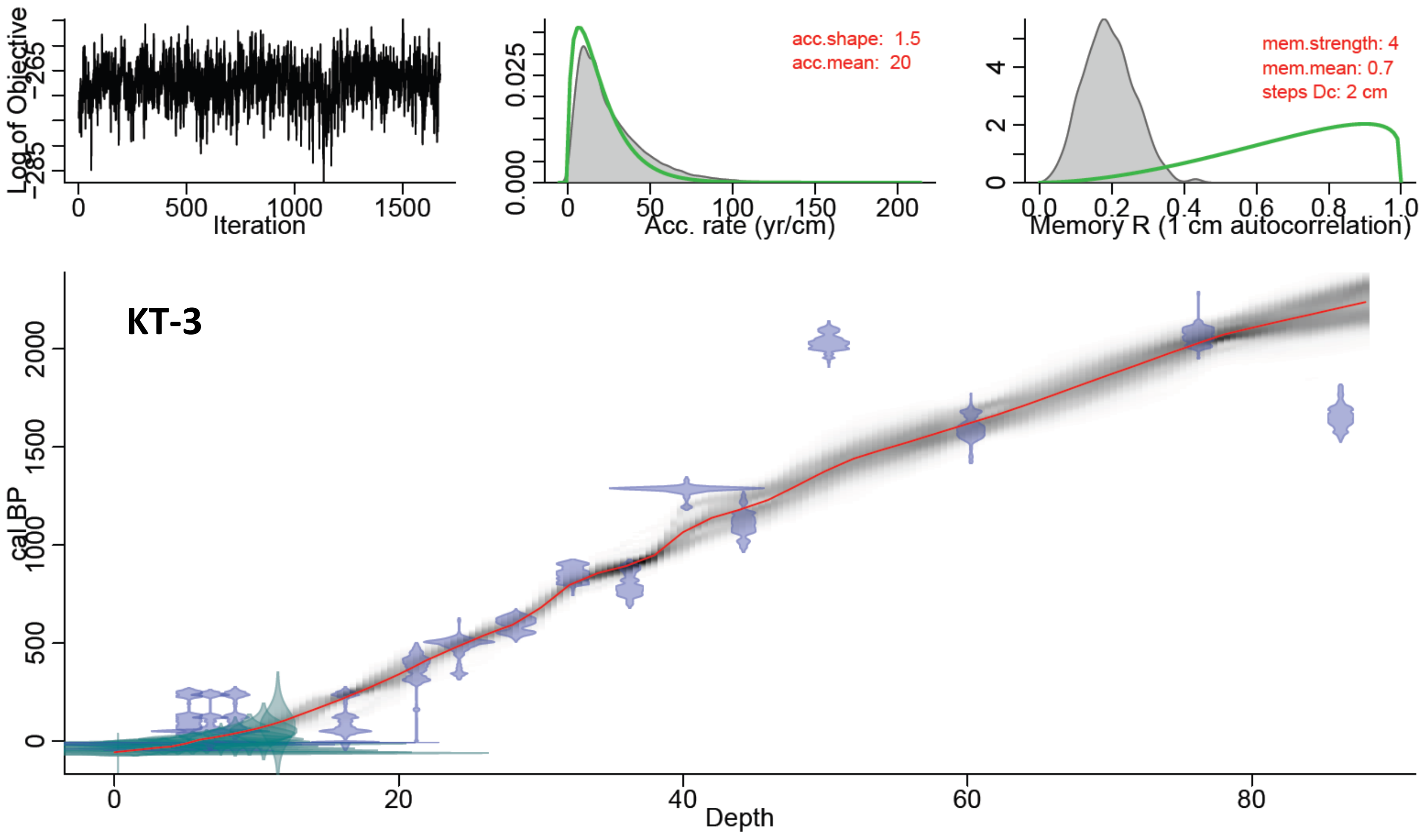

Supplementary Figure 7

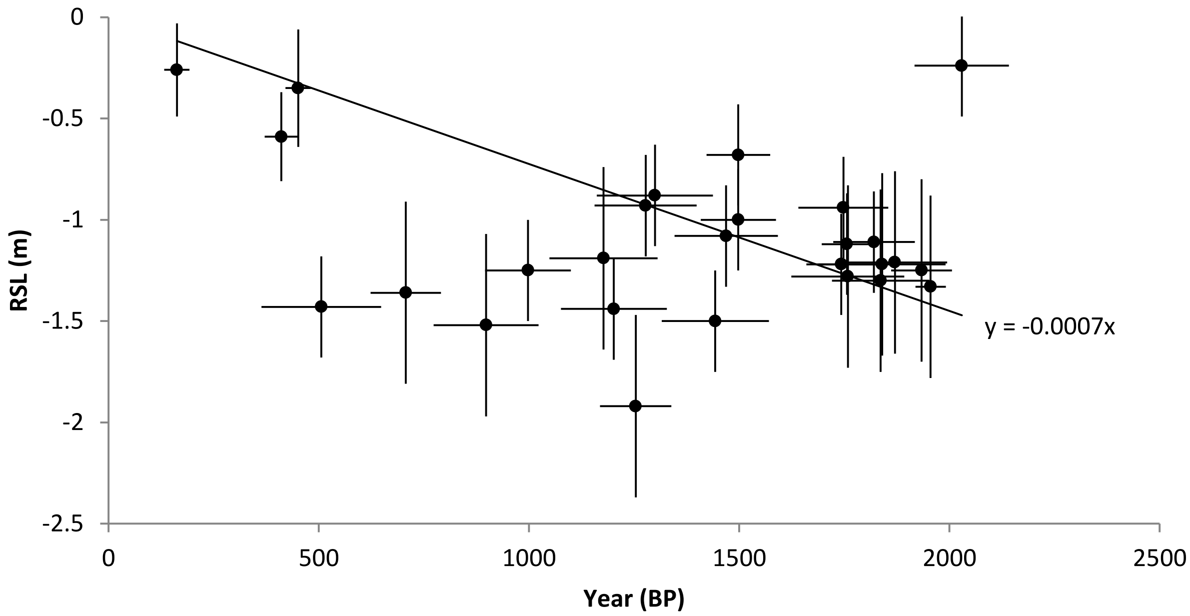

Supplementary Figure 8